

LBL-11446  
EEB-W-80-14  
W-70

Submitted to Solar Energy Materials

HEAT-MIRROR COATINGS FOR ENERGY-CONSERVING WINDOWS

Carl M. Lampert

Materials and Molecular Research Division  
and  
Energy and Environment Division  
Lawrence Berkeley Laboratory  
University of California  
Berkeley, California 94720

August 1981

The work described in this paper was supported by the Assistant Secretary for Conservation and Renewable Energy, Office of Buildings and Community Systems, Buildings Division of the U.S. Department of Energy under Contract No. W-7405-ENG-48.

This work was conducted as part of the Lawrence Berkeley Laboratory's Windows and Daylighting Program with support provided by the U. S. Department of Energy. For further information regarding related program activities, please contact:

Windows and Daylighting Program  
Building 90, Room 3111  
Lawrence Berkeley Laboratory  
University of California  
Berkeley, California 94720  
(415) 486-5605

# HEAT-MIRROR COATINGS FOR ENERGY-CONSERVING WINDOWS

Carl M. Lampert

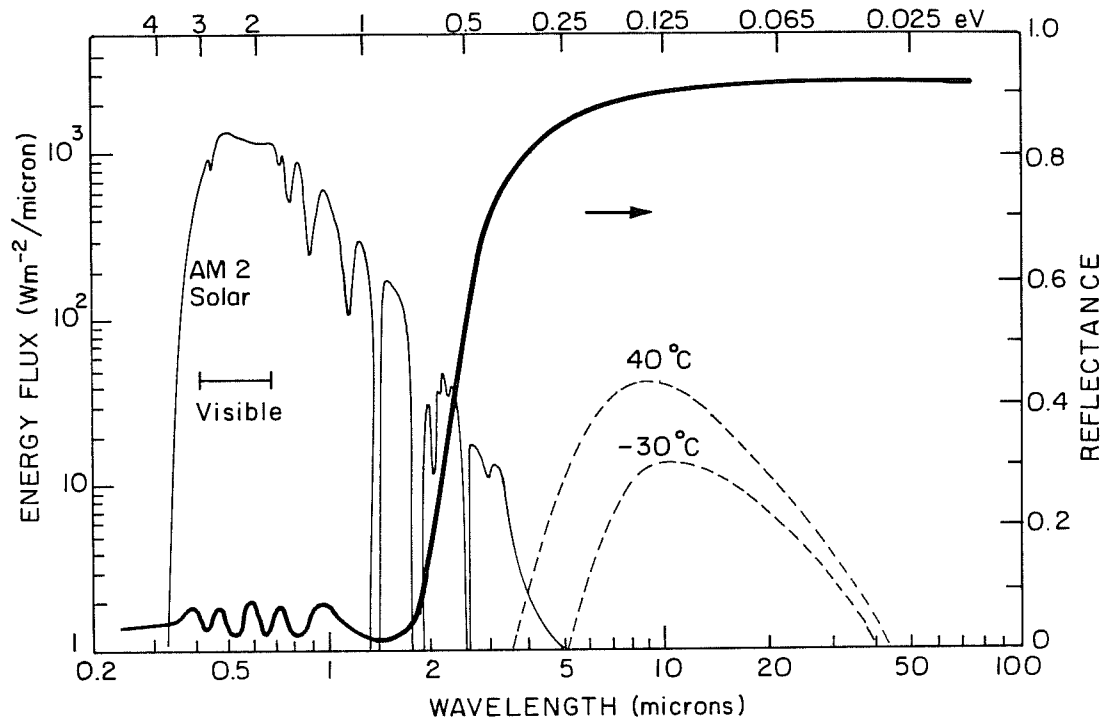
Materials and Molecular Research Division  
and  
Energy and Environment Division  
Lawrence Berkeley Laboratory  
Building 62, Room 235  
University of California  
Berkeley, California 94720

August 1981

Abstract. Heat-mirror coatings are important as transparent insulation for a host of applications, including building window glazings. They reduce thermal emittance of glass and polymeric substrates, thereby decreasing the effective radiative loss of a glazing or window assembly. Properties of coatings and substrates, as well as various window designs, are detailed. The paper reviews heat-mirror deposition technology including chemical vapor deposition using hydrolysis and pyrolysis reactions, DC and RF sputtering using reactive, biased, and nonreactive techniques, vapor deposition, and ion plating. The properties of single-layer films including coatings of  $\text{In}_2\text{O}_3:\text{Sn}$ , doped  $\text{SnO}_2$ ,  $\text{Cd}_2\text{SnO}_4$ , noble and transition metal films are enumerated. Multilayer films described include dielectric overcoated metals such as  $\text{ZnS/metal/ZnS}$ ,  $\text{Bi}_2\text{O}_3/\text{Au/Bi}_2\text{O}_3$ , and  $\text{TiO}_2/\text{Ag/TiO}_2$ . Electrical, solar, and infrared radiative properties are tabulated. Much of the data presented is also useful for photovoltaic and collector applications. New and innovative materials systems are suggested.

## I. INTRODUCTION

Heat mirror coatings can be used successfully for a variety of window<sup>1,2</sup> and solar-collector<sup>3,4,5,6</sup> applications. Other uses are in photovoltaic,<sup>7</sup> electronic, lighting,<sup>8,9</sup> electro-optical, and industrial heat shielding, aircraft, spacecraft,<sup>10</sup> and vehicle applications. Details of application and performance of heat mirrors for building windows are reviewed elsewhere,<sup>1,11,12,13</sup> including commercial and marketing analyses.<sup>14</sup> There are, however, some basic considerations that need to be explained to put these coatings in the proper context for energy efficient windows. In this study, "heat mirror" is defined as a wavelength selective coating exhibiting appropriate reflectance or transmittance for radiant energy in three portions of the electromagnetic spectrum. These regions are high-energy solar (HES) (including the visible) 0.3-0.77 microns, near-infrared (NIR), 0.77-2.0 microns, and infrared (IR), 2.0-100 microns. Heat mirrors generally exhibit medium to high transmittance over the visible and high reflectance (or low emittance) throughout the infrared. The properties for the near-infrared vary according to design and application. A simplified solar spectrum with two superimposed black body spectra is shown in Fig. 1, along with a heat mirror wavelength response. It provides the relationship between wavelength and incident flux for a given air mass. For the air mass two solar spectrum, the energy content is roughly split between the visible and near-infrared regions. For all heat mirror designs for building applications, the coating provides a low-emittance surface, where the net effect is to



XBL 808- 5758B

Fig. 1. Air mass two solar spectrum with two black body spectra ( $40^\circ\text{C}$ ,  $-30^\circ\text{C}$ ). Superimposed is the idealized reflectance of a tin dioxide heat mirror coating.

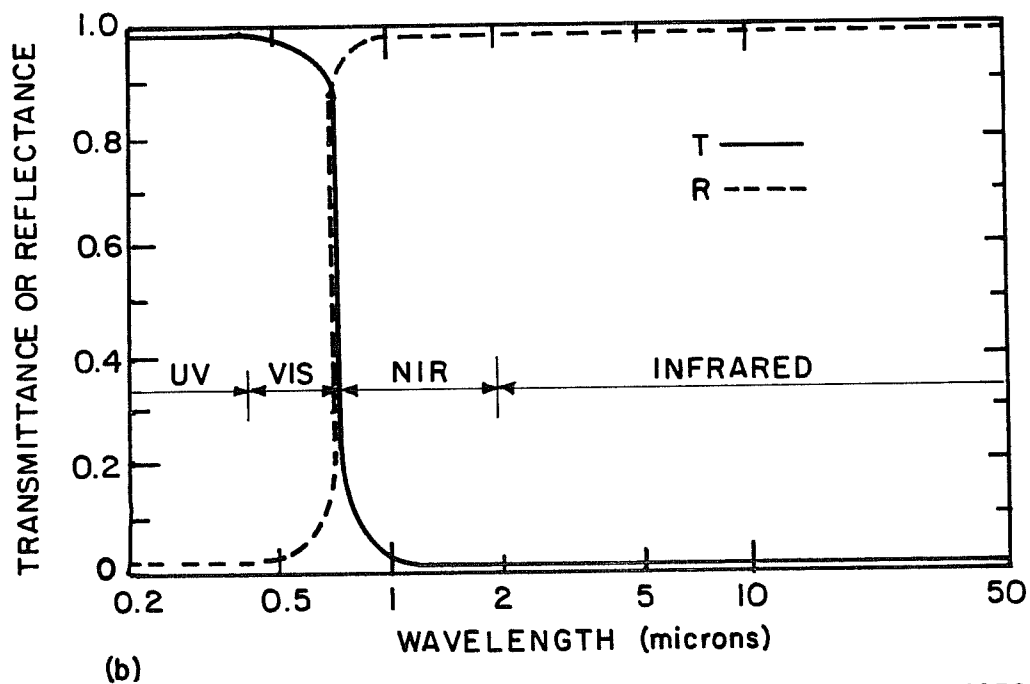
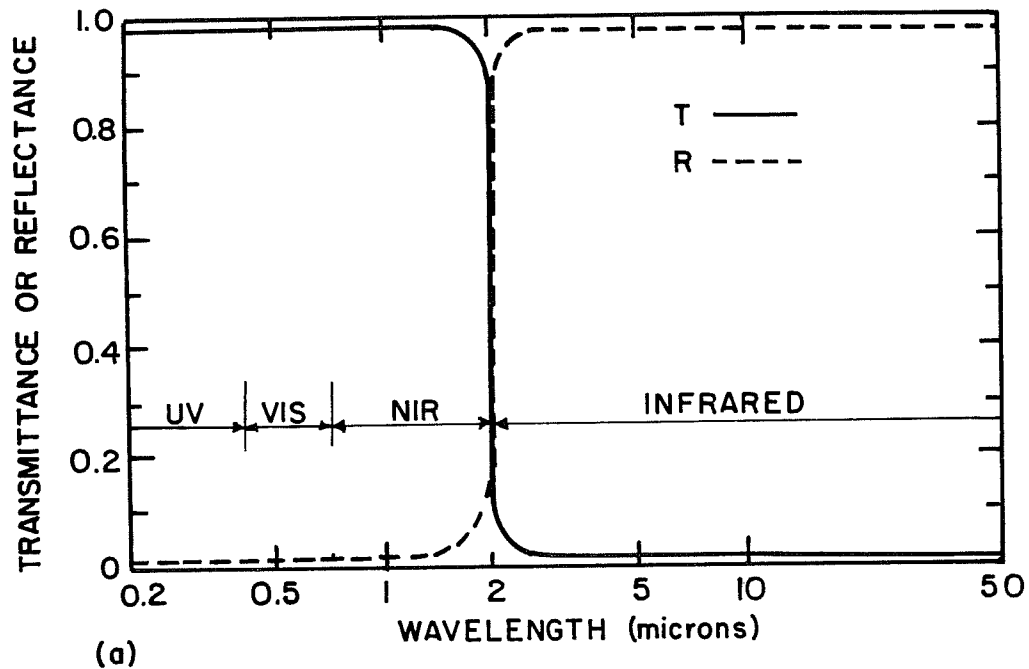
reduce heat transfer between the coated glazing layer and the environment, other glazing layers, and the room interior. The magnitude of reduction will depend on the nature and relative magnitude of convective and conductive heat losses.

Two scenarios can be invoked to demonstrate the usefulness of single glazed heat mirrors in buildings. The first scenario is for winter heating, where solar gain is important to reduce the building's heating load. The optimum heat mirror would act to transmit both solar visible and near-infrared to approximately a wavelength of 2 microns, as shown in Fig. 2A. The thermal infrared would be reflected back into the building. In this fashion, the majority of the sun's energy could be utilized for daylighting and passive heat gain. Examples of this type are shown in Fig. 3.

The second scenario can be treated as a cooling load reduction heat mirror, where all infrared energy is reflected to reduce air-conditioning thermal loads. A heat mirror of this type must have the basic property shown in Fig. 2B. This coating allows visible energy to be transmitted through the window, while the majority of all infrared including that of the sun is reflected away from the building, as shown in Fig. 4.

In the models shown in Figs. 3-5 only generalized reflections are detailed. A more exact study has been done recently.<sup>15</sup> All surfaces should exhibit a finite reflectance. One also expects partial transparency of some substrates over 2-5 microns. In addition, to complete the models the effects of convective and conductive heat

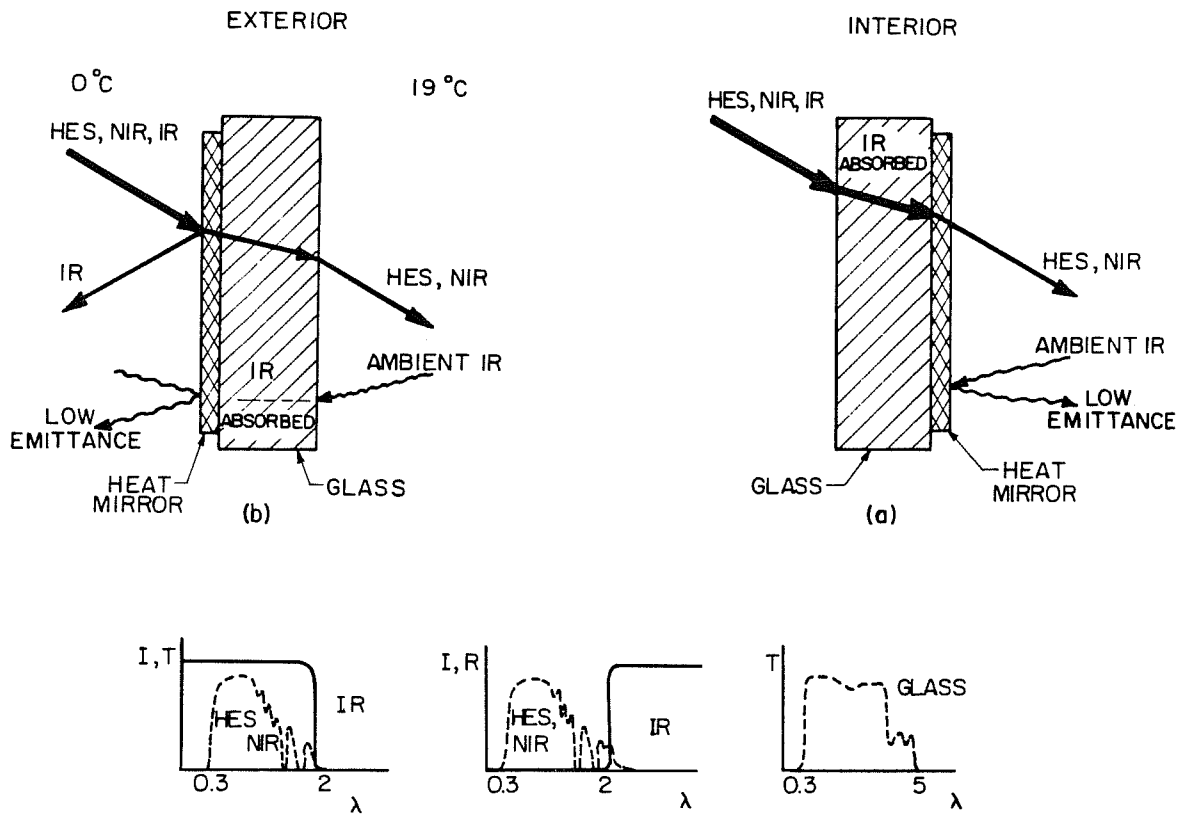
## IDEAL HEAT MIRROR SPECTRAL RESPONSES



XBL 817-6038

Fig. 2. Idealized heat mirror wavelength responses. Both heating load ( $T_1$ ,  $R_1$ ) and cooling load ( $T_2$ ,  $R_2$ ) heat mirror characteristics are depicted, respectively, in Figs. 2a and 2b.

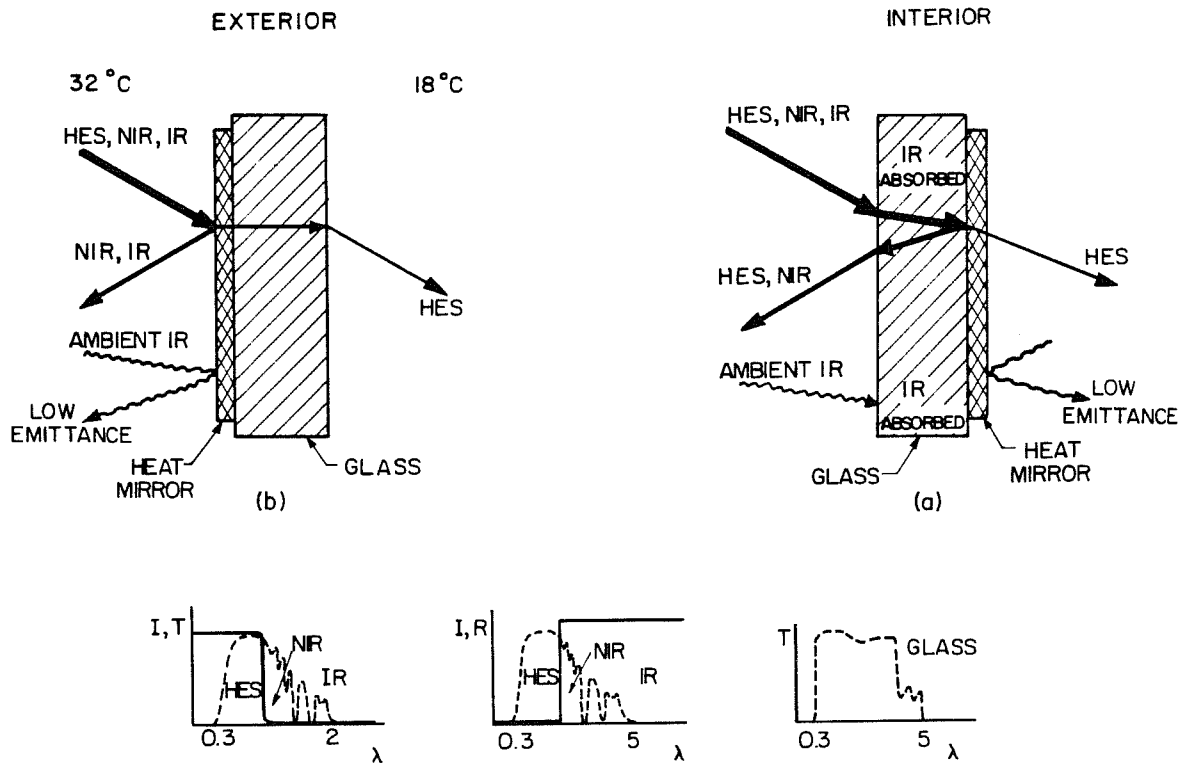
## HEATING LOAD HEAT MIRROR



XBL 811-7731

Fig. 3. Schematic of heating-load interior and exterior heat mirror properties. Inset shows the solar spectrum and how coating reflects infrared energy. Also, the transmittance of glass is shown. The exterior placement is subject to convection losses which lessen the heat mirror effect.

## COOLING LOAD HEAT MIRROR



XBL 811-7732

Fig. 4. Schematic of interior and exterior single glazed heat mirror demonstrating the properties required to reduce cooling loads. Inset shows relationship of solar spectrum to reflectance and transmission of glass. The exterior placement is a poor design because of potential convection losses.

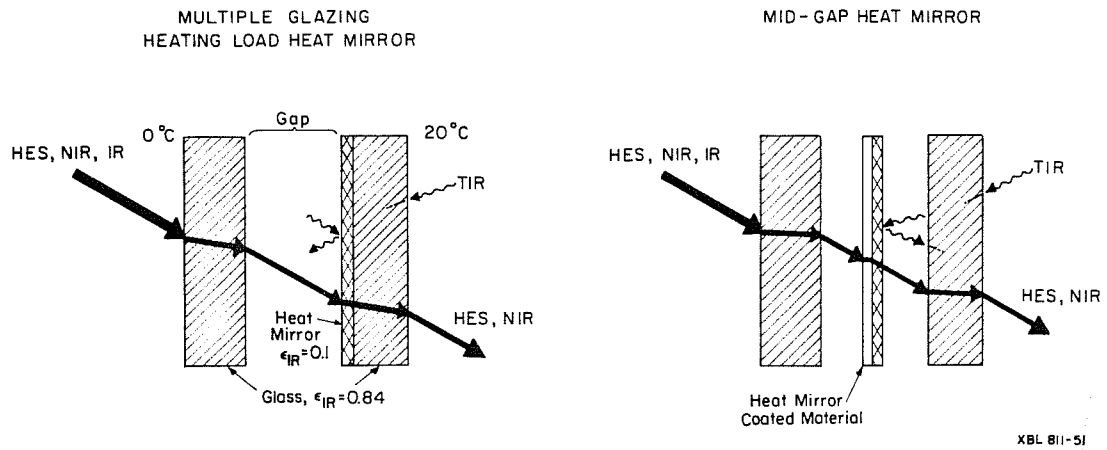


Fig. 5. Two multiple glazed windows incorporating heat mirrors  
Both configurations have properties of high solar  
transmittance, low infrared emittance, high infrared  
reflectance.

transfer must be accounted for. Proper placement of the heat mirror coating in a glazing is important to achieve the maximum benefit. For examples, In Figs. 3b and 4b exterior placement is a poor choice. These configurations are useless in moderately windy conditions because convective losses overwhelm any decrease in radiative losses the heat mirror would provide. In actual designs, orientation, climate, and building type are important factors in choosing coating parameters. In some cases, intermediate scenarios and heat mirror transmittance and reflectance properties would be optimal.

In practice, heat mirrors can be used in double and multiple glazing applications as shown in Fig. 5, hence the models become more complex. Figure 6 shows the results of computer modeling,<sup>13</sup> effect of multiple glazing, and coating placement with overall thermal conductance, or U value. For comparison, an insulated outside non-glass wall might have a conductance of the order of  $0.6 \text{ W/m}^2\text{K}$  (R 11) to  $0.3 \text{ W/m}^2\text{K}$  (R 19). A triple-glazed optimized window panel might consist of two outside glass sheets with an inside heat mirror coated sheet. All sheets would be separated and the space filled with a low-conductivity gas. The inner sheet could be a thin polyester, polyethylene, or polypropylene material. The thermal conductivity for such a panel has been estimated<sup>16</sup> as  $U = 0.74 \text{ W/m}^2\text{K}$ . A commercial double-glazed window coated with dielectric/gold multilayers<sup>17</sup> has overall values of  $T_{\text{vis}} = 0.66$ ,  $T_s = 0.44$ , and  $R_{\text{ir}} = 0.7$  (2 microns), which is fair considering that an uncoated single glazing has  $T_{\text{vis}} \sim 0.90$  and double glazing  $T_{\text{vis}} \sim 0.8$ .

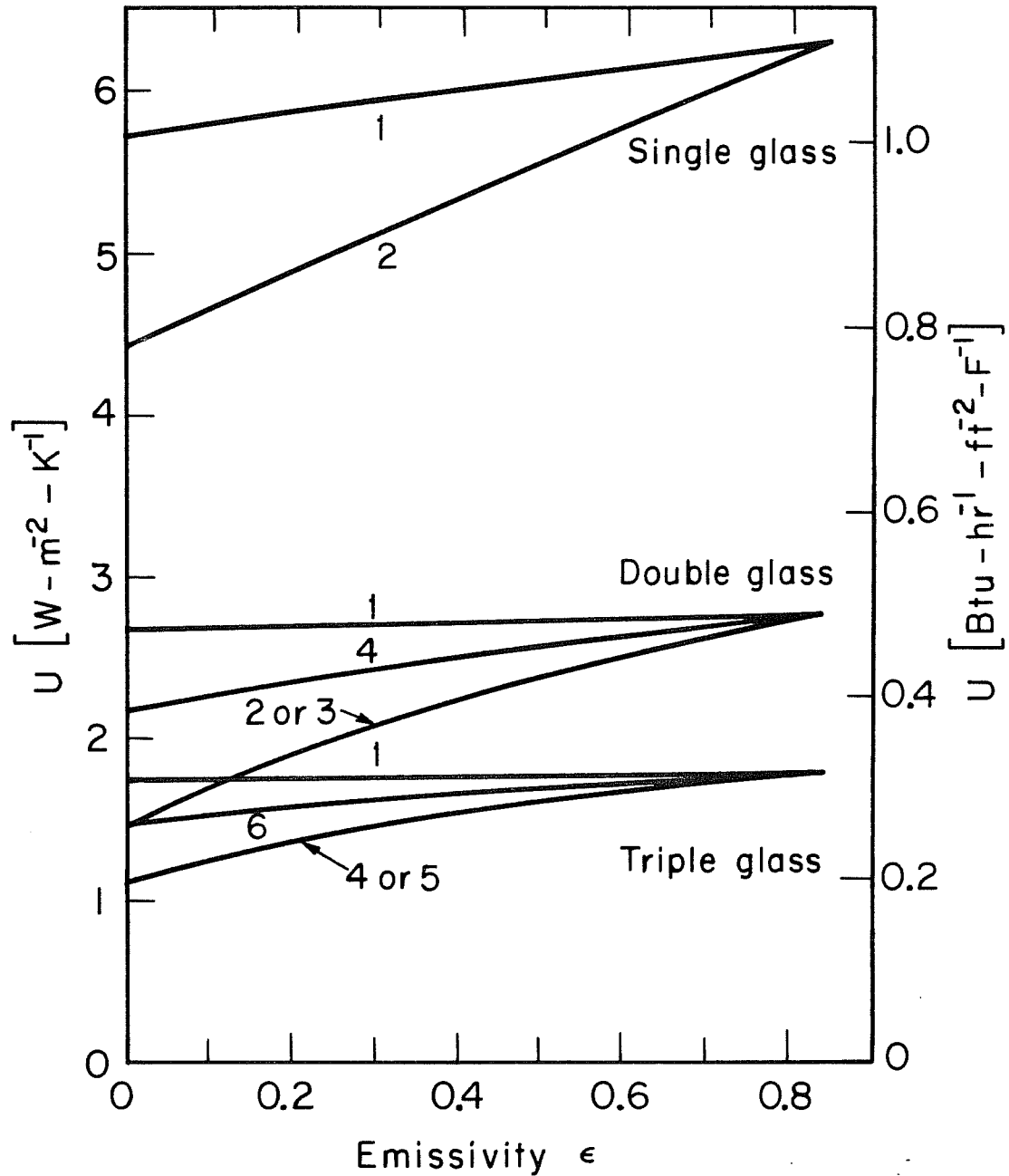
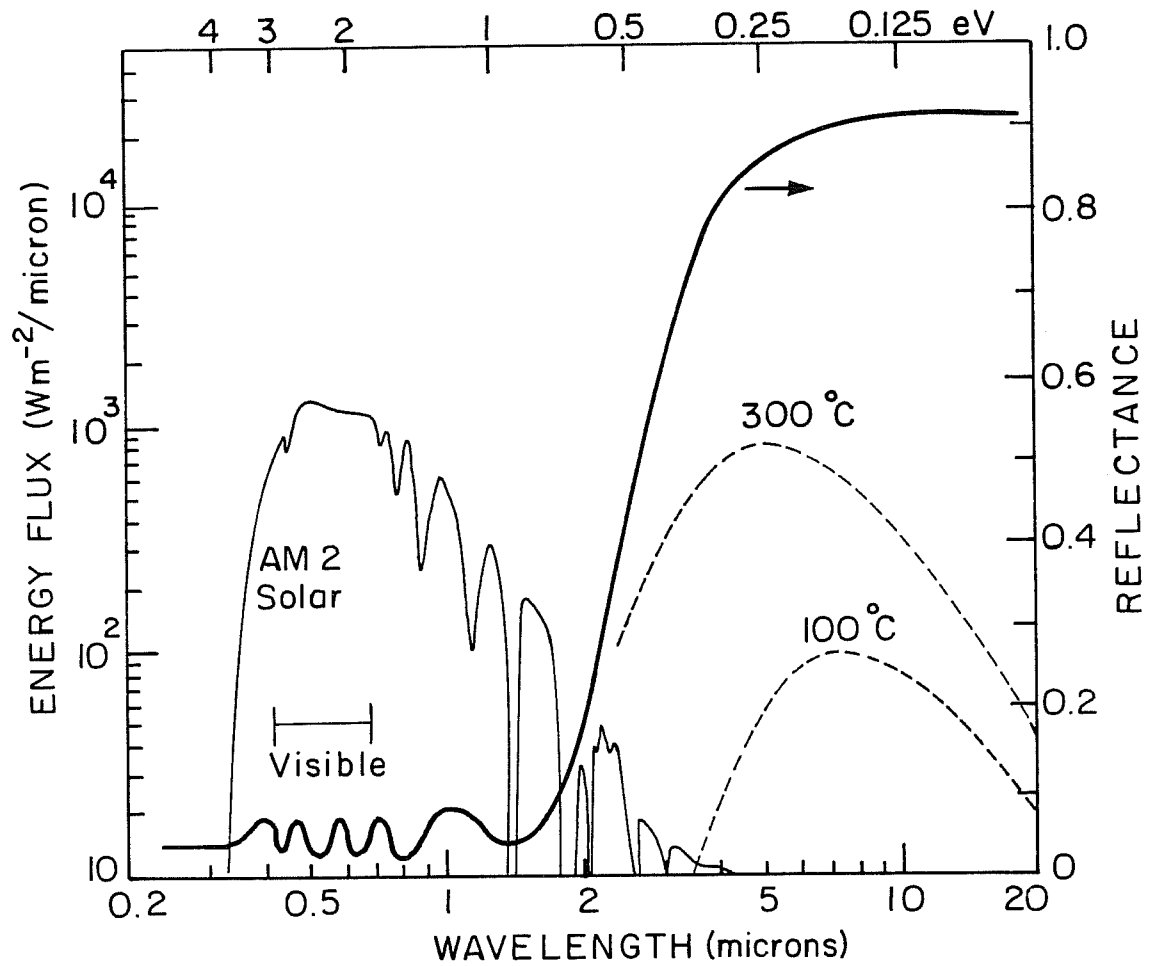


Fig. 6. Computer modeled U-values derived under ASHRAE standard winter conditions ( $T_{\text{OUT}} = -18^\circ\text{C}$ ,  $T_{\text{IN}} = 18^\circ\text{C}$ , wind speed 24 Km/hr). Plots are for single, double, and triple glazing. The effect of lowering the emittance of a glass surface by adding a heat mirror coating is detailed. The surfaces on which the heat mirror appears are given as consecutive numbers, starting from the outside surface labeled 1. For multiple glazings, each air gap between

A type of heat mirror similar to that of the heating-load design could also be used for solar thermal collectors. One modification might be to shorten the transition or cutoff wavelength to be more suitable for high operating temperatures of solar collectors. This is necessary, since the thermal radiation spectrum of a collector or cavity receiver corresponds to a higher temperature than that of a building, as shown in Fig. 7. For example, transition wavelength might be at 1-1.5 microns for a collector. Also, for collectors, thermal stability of the heat-mirror coating is a prime consideration. When using heat mirrors for high-temperature (540-1650°C) cavity receiver windows, a theoretical efficiency of 20-30 percent can be realized.<sup>18</sup> The majority of data presented here is generalized so that it is useful in architectural and solar applications amongst other diverse uses.

An important consideration in designing an optimum heat mirror is to correlate the tradeoff between visible transmittance ( $T_{vis}$ ), and infrared reflection ( $R_{ir}$ ), or infrared emittance ( $E_{ir}$ ). This is important not only from the standpoint of material processing capabilities, but from a solar gain (daylighting) versus  $R_{ir}$  or higher insulating (lower U value) tradeoff. Not until a range of values for  $T_{vis}$  or solar transmittance ( $T_s$ ) and  $R_{ir}$  are specified can this optimization be carried out with confidence. The toughest situation to satisfy would be where both substantial winter-heating and summer-cooling loads existed. A film with reversible or variable properties (such as photochromic, thermochromic, or electrochromic materials) would be best

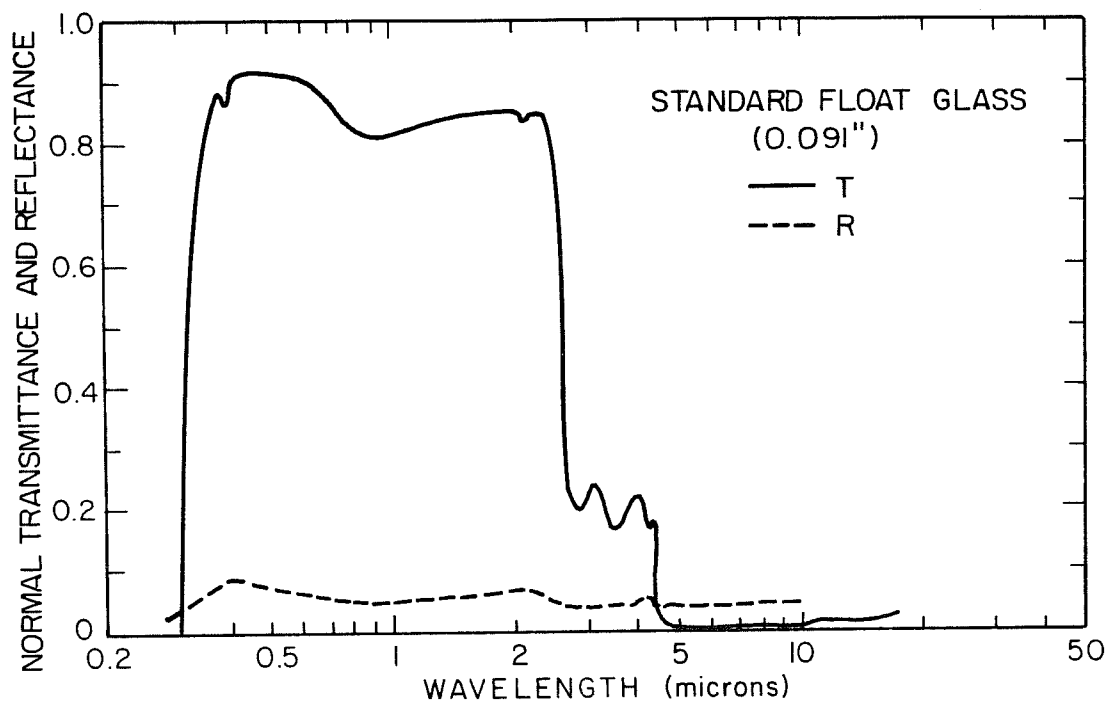


XBL808-5757A

Fig. 7. Air mass two solar spectrum with two black body spectra (300°C, 100°C), which might be appropriate to model solar thermal conversion. Also plotted is the reflectance properties of a tin dioxide film.

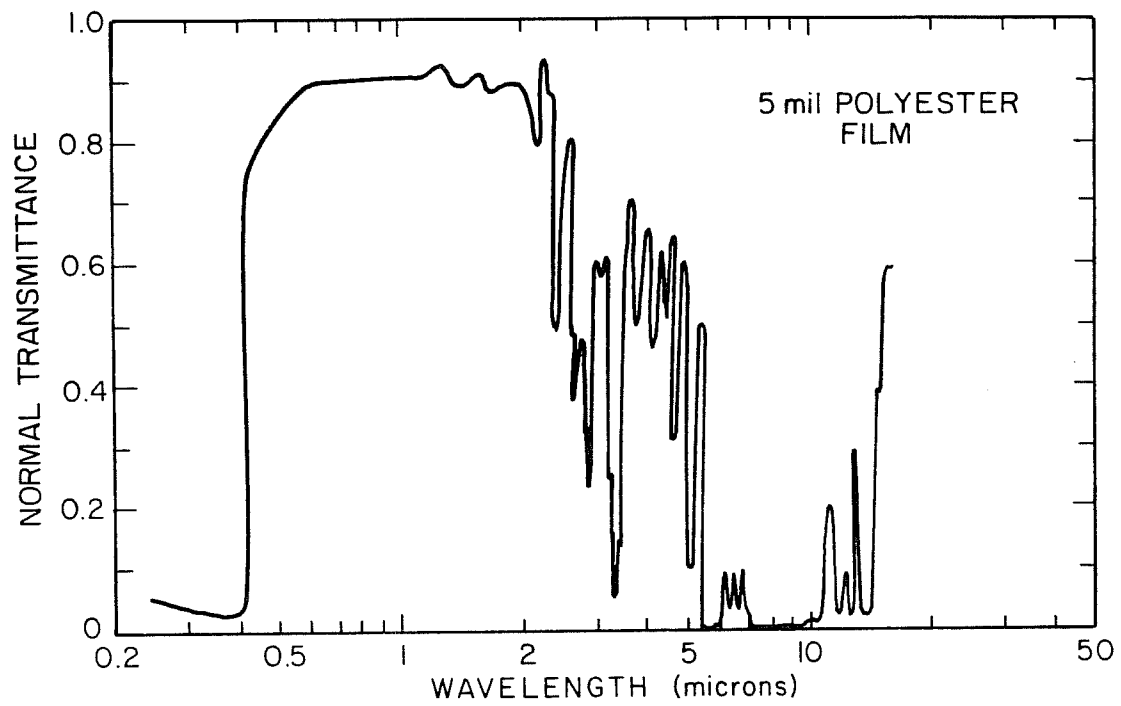
for this case. Of course, the seasonal fuel availability and regional economics would dictate the proper solution.

Both glass and some plastics are used as substrates or as intermediate materials. Due to this fact, it is important to know the properties of these materials as well as how they influence the nature of the heat mirror layer. In Figs. 8-12 are shown representative optical transmission graphs of glass and plastic substrates. It is essential for the designer to note that infrared properties are as important as the visible ones. Basically, these materials appear absorbing in the infrared; however, some thin-film materials can be partially transmitting or in a few cases exhibit low or localized absorption in the infrared. A heating load heat mirror on this type of plastic substrate would transmit high energy infrared, decreasing the U value of the sandwich. Some plastics such as polycarbonate exhibit a nonspecular (diffuse) component to their transmittance, which tends to decrease optical clarity. Also, the stability and mechanical properties of substrates must be considered since they can dictate the suitability and lifetime of the sandwich structure. Ion plating has been used to apply stabilizing coatings of  $TiO_x$  and  $SiO_x$  to polyester and polyethersulphone.<sup>19</sup> A dendritic metal-oxide coating has been successfully used to visibly antireflect polyester film. This high solar transmission ( $T_S = 0.94$ , UV stabilized, 0.004") film can also be used as an inner glazing material where the properties of a heat mirror are neither desirable nor appropriate.<sup>20</sup>



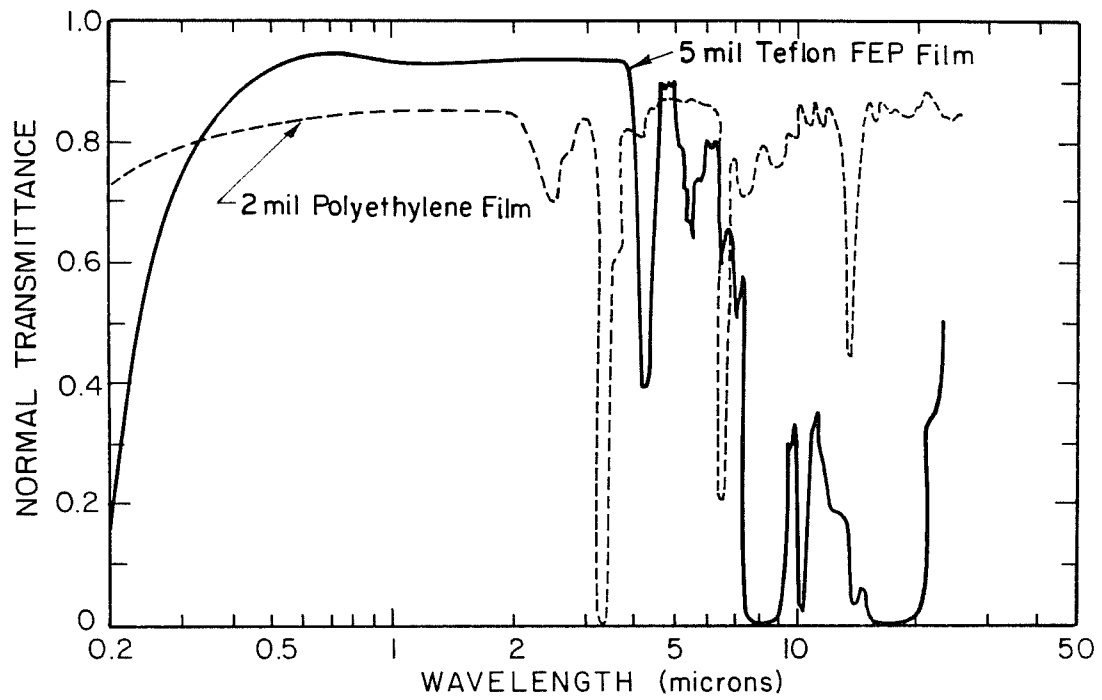
XBL 809-5844A

Fig. 8. Normal transmittance and reflectance of a typical float glass (single strength).



XBL 809-5845A

Fig. 9. Normal transmittance of polyester film.



XBL 809 - 5847 B

Fig. 10. Normal transmittance of teflon FEP and polyethylene films.

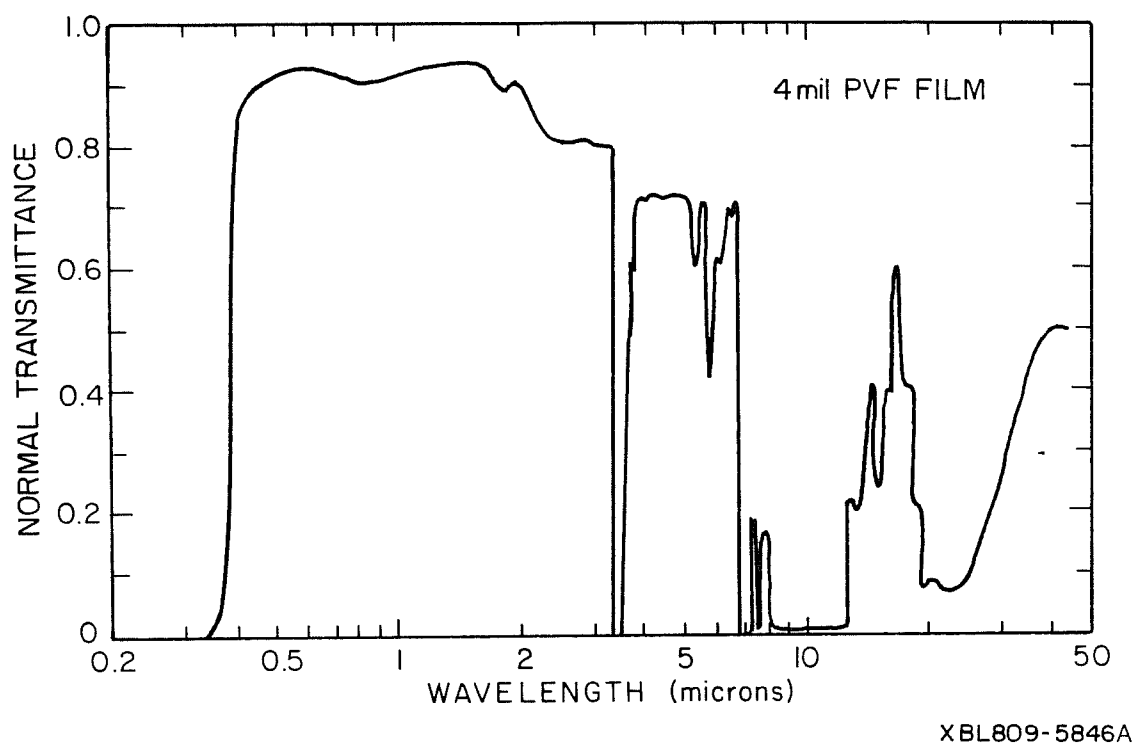
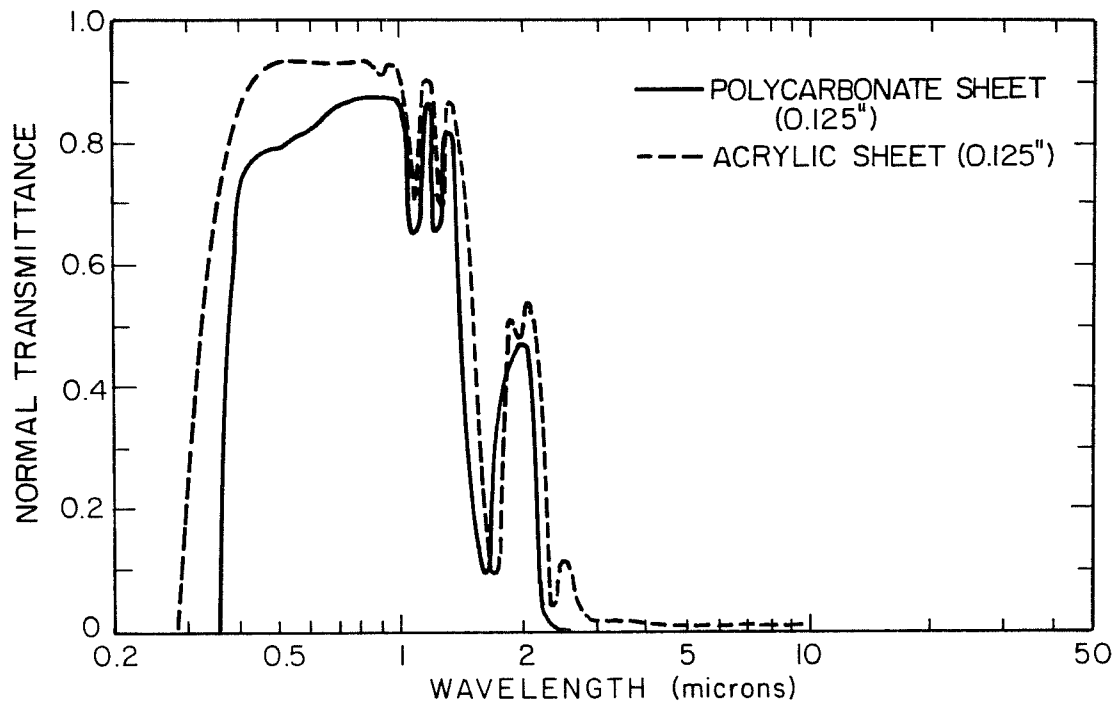


Fig. 11. Normal transmittance of polyvinyl fluoride film.



XBL809-5843A

Fig. 12. Normal transmittance of polycarbonate and acrylic sheet materials.

Another class of coated glazing product that should be mentioned in passing are those known as solar-control films. These are essentially nonselective films, which can be on glass or polymer substrates, and which have a relationship to heat mirrors similar to that between selective and nonselective absorbers. Solar-control films offer solar reflectance at the expense of visible transmission. However, solar-control films do provide a necessary function when significant reduction of visible transmittance and glare are prescribed. There are presently efforts by manufacturers to develop solar control films with wavelength selective properties more like transparent heat mirror films. By the use of infrared transparent polymers on thin metal coated substrates, a heat mirror effect can be created. This idea is akin to the dielectric/metal concept. Infrared transparent polymers of the general categories of polyethylene, polyvinylidene chloride, polyacrylonitrile, polypropylene, and polyvinyl fluoride might be used along with thin films of other polymers. Many of these materials are used for infrared physics applications.

Deposition technology is very important from the viewpoint of heat mirrors as cost-effective products. While the ultimate heat mirror deposition procedure might be a simple dip or spray (this probably would be performed commercially due to the low optical distortion or uniformity required of many window systems), no currently existing methods have the proper requirements. However, a promising technology for dipping glass has been developed by Schott Glass for solar control glass.<sup>21</sup> Various types of deposition technologies, including chemical vapor deposition (CVD) and physical vapor deposition (PVD) will be covered briefly in the following section.

## II. DEPOSITION TECHNOLOGY

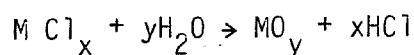
The electrical and optical properties of heat mirror films are directly related to the exact chemistry and physical morphology of the coating. Oxide coatings depend heavily upon stoichiometry, impurities, and defects in the films. Metal films are very dependent upon nucleation and coalescence phenomena (supersaturation, undercooling, interfacial energy, and impurities). In all films, the degree of crystallinity, crystal structure, and impurities influence both electrical and optical conductivity. Due to these interrelationships, different deposition techniques or even alterations of a fixed technique can result in a vast range of film properties. Deposition techniques for heat mirrors cover both reactive and nonreactive techniques of chemical vapor deposition; evaporative physical vapor deposition (also known as vapor plating), magnetron sputtering, ion sputtering, electron beam evaporation, and ion beam plating (plasma-assisted processes).

In all deposition processes requiring high substrate temperatures or high electron or ion influence, alkali element diffusion can be a serious problem. In general, float glass is avoided as an experimental substrate; quartz or low-alkali glass is used. Also, high-temperature heat treatments induce the diffusion and reaction of alkaline ions under certain conditions. This is a limiting factor for the production of heat mirror on float glass of varying and generally uncontrolled composition, and limits the usefulness of a number of deposition processes. Typical plastic substrates, on the other hand, are limited to processes below approximately 100–250°C. At elevated temperatures plastics can soften,

thermally expand or contract making processing difficult. Furthermore, many plastics suffer from oxidation, loss of plasticizer, decomposition, and reduction of strength at higher temperatures.

#### A. Chemical Vapor Deposition: Hydrolysis

Chemical vapor deposition encompasses a wide range of gaseous chemical reactive techniques and apparatus. A simple form of CVD is hydrolysis of metallic chlorides, which has been used to make films principally of  $\text{SnO}_2$  and  $\text{In}_2\text{O}_3$ . The overall reaction is as follows:

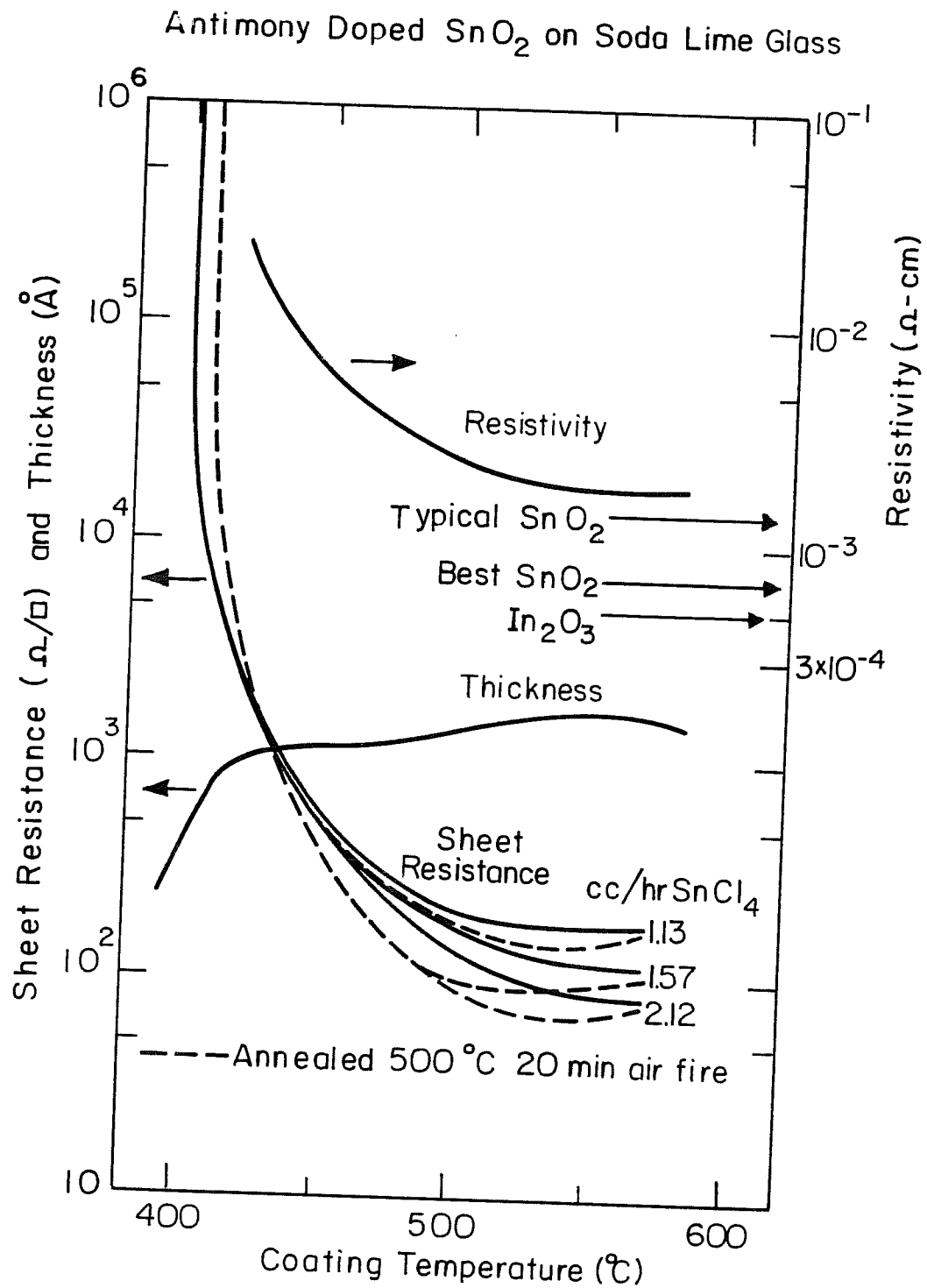


Also, a solvent delivery vehicle, such as alcohols or organic acids, is used. These solvents also act to create a reducing atmosphere during deposition, resulting in oxygen deficient films. Pyrogallol has been used for reduction.<sup>22</sup> The substrate temperature determines the amount of chloride doping; high temperatures favor less doping and greater oxide reduction. This technique is suited principally to glass substrates since high temperatures are required. Alkaline impurities (p-type) are generally found in oxide deposits, originating from the substrate. Films are formed by either spraying or dipping of component reagents on heated (400–800°C) substrates. The major weaknesses associated with this technique is substrate warping due to thermal gradients, diffusion of substrate impurities, poor extraction of HCl by-product, and the high energy input required for heating. Recently, a CVD conveyor furnace has

been reported.<sup>23,24</sup> It can potentially enhance processing time, quality control, and soften thermal gradients. The properties of CVD films are shown in Fig. 13.

#### B. Chemical Vapor Deposition: Pyrolysis

Pyrolysis is the thermal decomposition of an organometallic or metal salt reagent in the presence of oxygen over a heated substrate. A carrier gas such as argon, along with substrate temperature, is used to regulate reaction rate. Both of these parameters must be controlled to inhibit gas phase nucleation resulting in powdery deposits. The major limitations of pyrolytic reactors are small areas of uniform deposition, and expense of organometallic feedstock. In spite of this, the apparatus is relatively inexpensive in terms of capital equipment cost. In one case it was noted that substrates of soda-lime glass not only gave poor films but contaminated the reactor with alkaline elements. Typically, low alkali or fused silica glasses are used with this technique.<sup>25</sup> Because of this, pyrolytic processes appear to be less favorable for coating float glass. A comforting note, however, is the recent development of a lower temperature fogging pyrolytic reactor, which can be used for a wide range of oxides.<sup>26</sup> Also, recent work on  $\text{SnO}_2\text{:F}$  has resulted in a coating with high mobility and conductivity which is compatible to float glass processing.<sup>27</sup> Pyrolysis processes are more sensitive to high alkali concentrations than hydrolysis processes. For the best films, low-alkali glasses should be used. There are, however, technical solutions that can be utilized to reduce or eliminate surface



XBL80IO-6108A

Fig. 13. Relationship of thickness, sheet resistance, and resistivity for  $\text{SnO}_2\text{:Sb}$  films on soda lime glass processed by a conveyor CVD furnace (after 23).

alkali in float glass. The surface can be processed by ion depletion, selectively etching alkali ions with acids to leave an  $\text{SiO}_2$  layer, or the glass can be precoated with  $\text{SiO}_2$ .

Optical thin films of materials including  $\text{In}_2\text{O}_3$  have been prepared on substrates held at room temperature using plasma-assisted pyrolysis on  $\text{In}(\text{CH}_3)_3$ . In another case, plasma-enhanced CVD yielded films of  $\text{SnO}_2\text{:Sb}$  with 1.5 ohm/sq sheet resistance with  $T_{\text{solar}} = 0.85$  deposited at rates up to 500 Å/min.<sup>36</sup> However, in this case the substrate was held at 350°C.

Another near-ambient (30°C) technique has been used recently to deposit  $\text{SnO}_2$  from the tetramethyl tin.<sup>37</sup> An RF-activated oxygen plasma was used to decompose the organometallic. This technique is capable of growth rates of 160 Å/min, which is higher than CVD rates. The use of organometallic reactants offers great potential for development. It also offers challenges to chemists to develop low-cost make-up processes and chemicals.

### C. Physical Vapor Deposition: Evaporation

Vacuum evaporation is a widely known process. A large number of materials can be evaporated in vacuum and condensed on cooled surfaces. Most materials are either boiled or sublimed by resistive, inductive, or electron beam methods. Vacuum pressures below  $10^{-4}$  torr are typically used. Due to the need for a vacuum system, evaporation systems tend to be more complex than CVD. Deposition rates can vary from as little as 0.001 Å - 10 Å/sec to above 1 micron/sec. For evaporation on

heat-sensitive substrates such as plastics, water cooling is required. Alloys and certain compounds tend to be difficult to evaporate due to incongruent melting, disassociation, or decomposition. Multiple source evaporation can yield a graded composition over a substrate. Large commercial roll and batch coaters have been fabricated and in use industry for coated plastics, paper, and metals for many years.

A modification to basic vacuum evaporation is reactive evaporation. Here a background pressure gas, such as oxygen, nitrogen, etc., is maintained to serve as a reacting atmosphere during evaporation. Oxide, nitride, etc., films can be formed in this manner. Also, their stoichiometry can be modified by pressure adjustments.

#### D. Physical Vapor Deposition: Sputtering

The major types of sputtering fall into the glow discharge or ion beam categories. The ion beam case will be treated later in this section. For glow discharge sputtering, two overall configurations exist: the diode and the triode types. Each type may employ DC or RF power sources. RF power enables the sputtering of nonconductive solids, since the power can be coupled through the target. Basic sputtering consists of a low-vacuum ( $10^{-2}$ - $10^{-3}$  torr) after high-vacuum ( $10^{-7}$ - $10^{-9}$  torr) outgassing in a chamber with an argon or inert fill gas. Accelerated argon ions (for example) in the form of a plasma are used to eject material from a target or source. This material traverses the plasma and intercepts the substrate. By RF plasma rectification or direct biasing, a strong negative potential is obtained on the target.

This charged target strongly attracts the positively charge ions. These ions have enough energy to drive off target atoms which arrive at the substrate at very high energies. It is because of this high-energy driving force that sputtered films have better adhesion than films made by other techniques. During this process the substrate may be grounded, floated, or biased. A floating substrate may be charged either positive or negative, depending solely upon deposition conditions. In general, a positive potential will decrease film density due to inert gas codeposition. A negative bias can increase purity by resputtering poorly bonded surface atoms. The film growth rate, quality, and character depend upon many factors including target voltage, target size, gas purity, target-to-substrate spacing, sputtering yield, bias, gas pressure, and substrate temperature. Deposition rates can range from several tens of angstroms to thousands of angstroms per minute.

To achieve high deposition rates, high ion densities are required. In simple discharge sputtering, only a small percentage of the plasma atoms are ionized. To increase efficiency, magnetron target geometries are used. These are essentially glow discharge sources that depend on crossed electric and magnetic fields to produce high ion densities giving high deposition rates, and minimal substrate bombardment by electrons. Magnetrons may be in planar or conical configurations, which have gradient magnetic fields, or cylindrical configurations in which the magnetic field is uniformly orthogonal to the electric field. In most of the systems detailed here, magnetrons are used. For large-scale high-rate processing of heat mirrors, magnetron technology is

necessary. Scale-up of a large sputtering plant from small laboratory equipment is a major engineering task. Such systems depend heavily upon configuration; getting uniform sputtering gas over large target areas, as well as uniform deposition, is one critical problem. However, in spite of this, large sputtering systems have been built commercially.<sup>39</sup>

RF sputtering of nonconductive compound targets can offer tight control of film stoichiometry so that high-temperature annealing is unnecessary.<sup>30</sup> One major problem with this type of target is that they are subject to contamination due to their porosity. Both  $\text{In}_2\text{O}_3$  and  $\text{SnO}_2$  are hygroscopic and susceptible to aqueous contaminants, resulting in the need for presputtering of the target. Other drawbacks with compound targets are fabrication expense and low sputter yields compared to metallic ones. Due to target heating, a target cooling system is required.

RF sputtering of oxide compounds in particular present some difficulty; for example, the act of sputtering a  $\text{SiO}_2$  target disassociates oxygen from silicon resulting in a substrate film that is deficient in oxygen. If it is desirable to preserve stoichiometry, oxygen can be bled into the system.  $\text{In}_2\text{O}_3$  can be RF sputtered at near room temperatures using oxide targets and a partial pressure of oxygen, giving highly conductive transparent films.<sup>30</sup> To increase the deposition rate, reactive sputtering is usually employed. Metals in general sputter faster than nonmetals. So the metal target is sputtered in an atmosphere of oxygen or mixed gases to give the desired oxide. Reactive sputtering can be used to form a wide range of compound films,

but film stoichiometry and process analysis is very difficult with this method. The dynamics of reactive sputtering of Sn-Sb and In-Sn alloys is not well understood.<sup>28</sup> Examples of reactive atmospheres to make films other than oxides include  $N_2$ ,  $H_2S$ ,  $CH_4$ ,  $H_2O$ ,  $C_2H_2$ , and  $NH_3$ .

Sputtering, in general, has better control of deposition rates than evaporation; also, sputtering is directional in nature, while evaporation is not, and generally wastes expensive source material. But sputtering has its drawbacks: it tends to be slower, pressure sensitive, and to require complex and expensive capital equipment. Magnetron sputtering inherently uses relatively lower substrate temperatures than evaporation, enabling a range of plastic substrates to be used. Evaporation requires more extensive substrate cooling for polymeric materials.

Alloy diffusion in targets of In-Sn and Sn-Sb is severe due to their low melting points.<sup>29</sup> Special measures must be taken to ensure alloy composition regularity. Under high-pressure reactive sputtering, a compound forms at the target surface and is consequently sputtered. Under low pressures, metal is essentially sputtered. During RF sputtering there is a lot of resputtering and preferential sputtering of the growing film. Frequently, in  $In_2O_3:Sn$  films there occur metallic inclusions during DC sputtering, so that an oxygen annealing procedure is specified to improve transmission. In many cases, the lowest film resistivities are obtained by subsequent heat treatment. Pure oxygen discharges have been used to decrease resistivity of  $In_2O_3:Sn$  films.

Ion beam sputtering is a process in which an ion beam of inert or reactive gas at high energy is directed at a target material which is sputtered onto a nearby substrate. In this fashion, better control over angle of deposition, bombardment and temperature of substrate is achieved. This technique is very useful to study film growth processes and morphologies. Deposition rates may be several hundred angstroms per minute.

Mylar (polyester) substrates have also been sputtered with  $\text{In}_2\text{O}_3:\text{Sn}$  ion beam sputtering in a reactive atmosphere.<sup>35</sup> In this case, use of an argon ion beam greatly reduced the level of electron bombardment seen by the substrate during RF sputtering. The net result was a relatively cool substrate (80°C).

#### E. Physical Vapor Deposition: Ion Plating

Historically, ion plating referred only to vacuum evaporation combined with a discharge, but now includes most processes where purposeful ion bombardment is performed during film growth. Generally, ion plating or ion-assisted deposition is a hybrid process in which material is evaporated (thermally or with an electron beam) or sputtered through a glow discharge to the substrate, which serves as the cathode of the discharge. In such a way, the deposited film is bombarded with ions and sputter etched during deposition. Reactive ion plating has been used to deposit various oxide heat mirrors on polyester substrates held at or near room temperature.<sup>31,32</sup> Film properties achieved by this technique

are similar to those of high-temperature sputtered films.<sup>33</sup> Ion plating combined with a roll coating apparatus can continuously deposit conductive oxides on PET film substrates.<sup>34</sup> This research unit can coat 10 cm x 250 m long substrates at a rate of 0.25 m/min. ITO films of 400 ohm/sq with  $T_{vis} = 0.9$  have been produced.

Other deposition techniques have been used to make transparent conductors. Fired metal resins, screen printing, electrostatic spraying, electroplating, anodization, diffusion, and fluidized bed coating have been used with some success for applications unrelated to heat mirrors. These systems have not been sufficiently exploited for heat mirror deposition to be evaluated.

### III. SINGLE-LAYER FILMS

It is generally known that solar transmittance and infrared reflectivity of single-layer semiconductor films are related by the free carrier concentration ( $N$ ) and film thickness. By increasing conductivity, infrared reflectance increases and the plasma frequency shifts to shorter wavelengths. At the same time, solar transmittance decreases due to increased absorption in the film. Absorption in the visible range is due to free charge carriers and lattice defects. To maximize transmission, the thickness must be as little as possible; but below a critical thickness the infrared reflectivity will be degraded. Other considerations are electron mobility ( $\mu$ ), effective mass ( $m^*$ ), and crystal lattice damping constants ( $g$ ). It is desirable to have high

mobility and DC conductivity ( $\sigma$ ) to insure proper infrared reflectivity. Along with this, free charge carriers and lattice absorption in the infrared (Reststrahlen bands) must be suppressed or shifted away from the peak blackbody wavelengths to be reflected. A very low lattice damping constant insures a rapid transition from low to high reflectance in the infrared. Refractory heavy metals have a high lattice damping constant, which results in a gradual transition from low to high reflectance. A figure of merit might be  $g/w_p$ , where  $w_p$  is the plasma frequency or transition frequency. It is desirable to have  $g/w_p \ll 1$ . Another figure of merit might be  $um^*$ , where a high product would favor minimum visible absorption and maximum conductivity. Other than materials such as  $\text{SnO}_2$  and  $\text{In}_2\text{O}_3$ , there is a potential for the high melting point lanthanide series hexaborides and alkali earth hexaborides such as  $\text{LaB}_6$  for being durable heat mirrors.<sup>40</sup> Little information is available about these materials and their optical properties. Materials like  $\text{CaB}_6$ ,  $\text{CuCl}$ ,  $\text{CuI}$ ,  $\text{MnO}$ ,  $\text{NiO}$ ,  $\text{SiN}$ ,  $\text{ZnO}$ ,  $\text{Sb}_2\text{P}_3$ ,  $\text{PbO}$ ,  $\text{SiTiO}_3$ ,  $\text{Cu}_2\text{O}$ ,  $\text{BaO}$ ,  $\text{Cr}_2\text{O}_3$ ,  $\text{BaTiO}_3$ ,  $\text{WO}_3$ , and incompletely filled d-shell materials such as  $\text{V}_2\text{O}_5$ ,  $\text{ReO}_3$ ,  $\text{Eu}_2\text{O}_3$  are all candidates for further materials research.<sup>41,42,43,44,179</sup> Currently, hard durable coatings of  $\text{TiN}$ ,  $\text{ZrN}$ , and  $\text{TaC}$  are being investigated as single-layer heat mirror coatings.<sup>45</sup> Various semiconductor heat mirror materials and processes prior to 1977 have been reviewed elsewhere.<sup>46,47,166</sup>

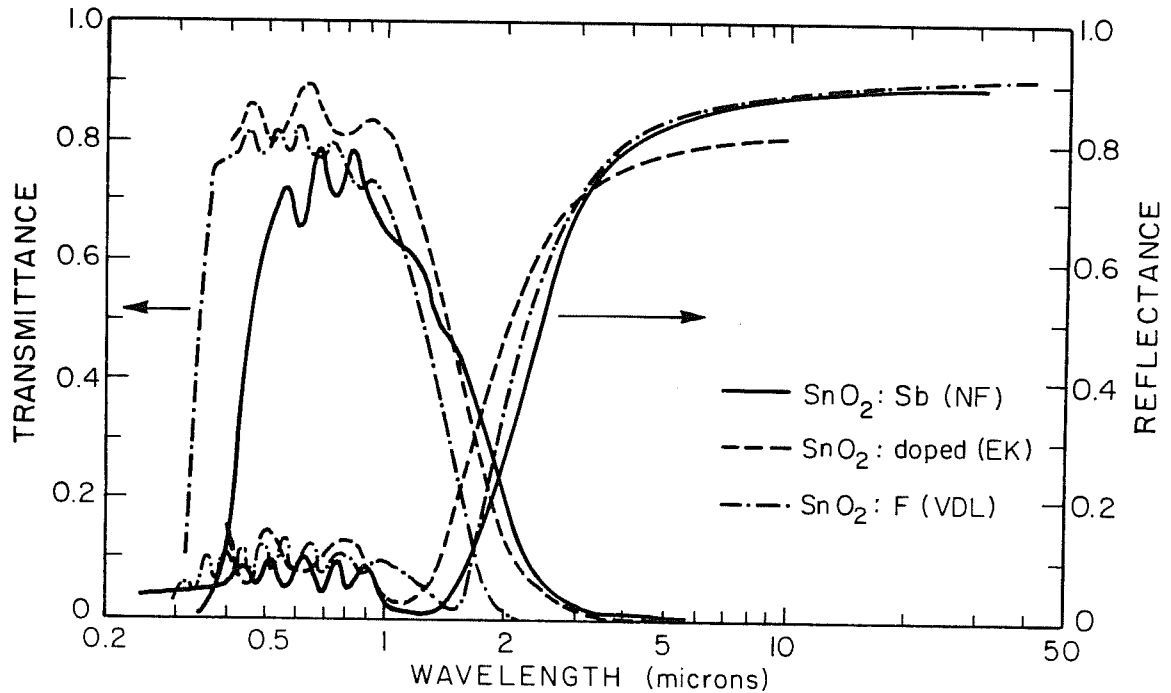
Doping is used to give high carrier concentrations to thin heat mirror films. A carrier concentration of  $10^{20}$ – $10^{21} \text{ cm}^{-3}$  corresponds roughly to an impurity-conduction band spacing of less than

0.3–0.4 eV. Another requirement of the impurity band is that it not be optically excited. Anion vacancies can have a similar effect. They can be induced by heat treating in specific atmospheres or by modifying the deposition parameters. To optimize a particular coating one must consider a  $T_S/R_{ir}$  ratio (solar transmittance to infrared reflectance ratio) along with the specific requirements and constraints of a window system. These specifications will weight the magnitude of both values of this ratio.

A very thin metal (100–200 Å) can also function as a heat mirror. Metals, and especially the noble metals Au, Ag, Cu, Ni, etc., offer high-bulk infrared reflectance. Very thin films are used to gain partial solar transparency. To further improve the transmission characteristics and durability, these films are overcoated with a dielectric or semiconductor which essentially acts to antireflect or suppress visible reflectance.

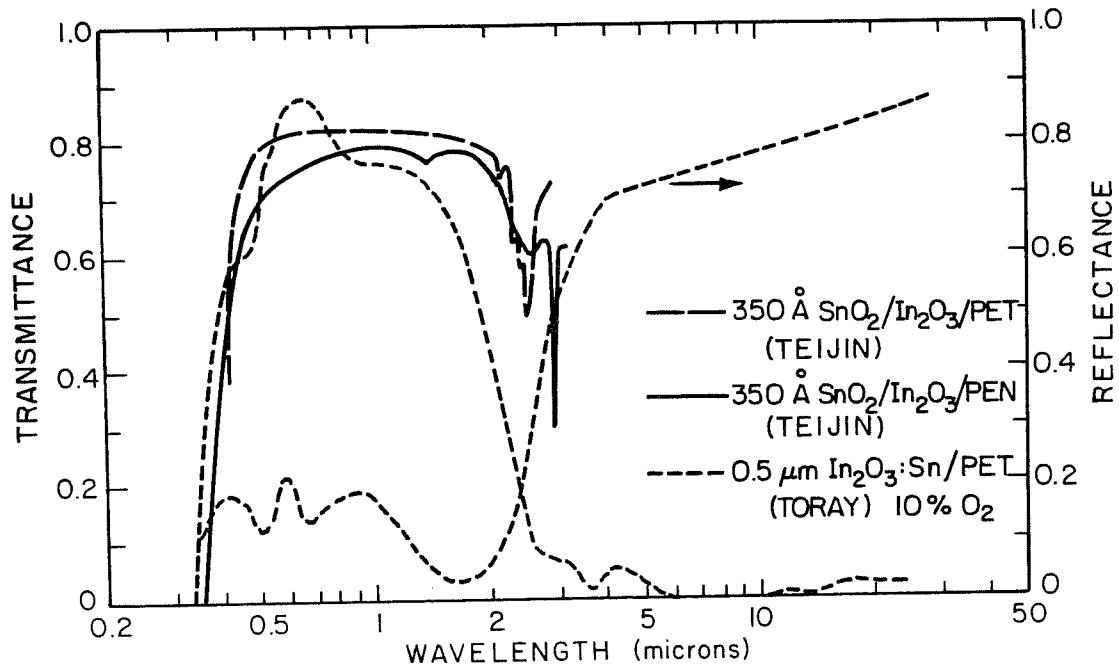
#### A. Transparent conductive oxides: Indium tin oxide

Both indium tin oxides, ITO ( $\text{In}_2\text{O}_3:\text{Sn}$ ), and doped tin oxides, ( $\text{SnO}_2:\text{Sb}$ ,  $\text{SnO}_2:\text{F}$ ), have very similar properties (see IIIB). Indium based films generally exhibit slightly superior infrared reflectance over tin oxides (see Figs. 14–16) due to higher electron densities and mobilities. However, indium oxides are dependent upon expensive and scarce indium feed-stock chemicals. The compound known as ITO is a tin oxide substitutional alloy of indium oxide, the tin being 5–10 percent atomically substituted. The presence of oxygen deficiency gives a film



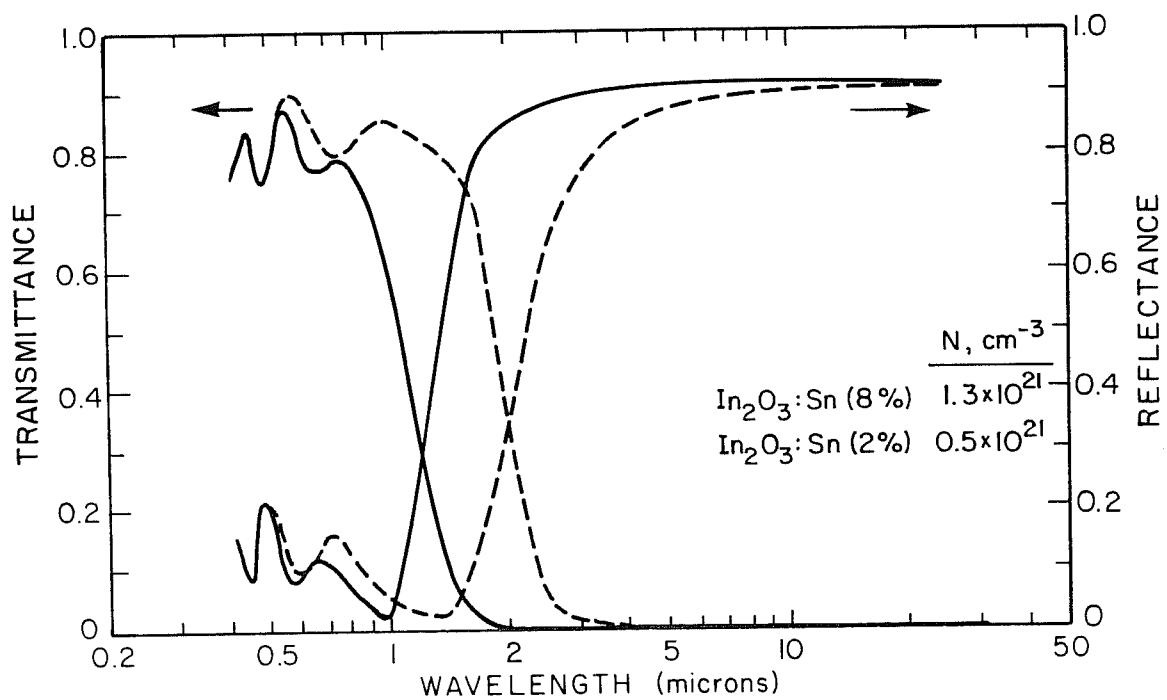
XBL 814-5505A

Fig. 14. Examples of several coatings of doped SnO<sub>2</sub> on glass. One layer (EK)<sup>132</sup> was formed by thermal decomposition of SnCl<sub>4</sub> at 460°C. The materials parameters are  $n = 6 \times 10^{20} \text{ cm}^{-3}$ ,  $t = 0.32 \text{ microns}$ ,  $E_g = 3.8 \text{ eV}$ ,  $u = 10 \text{ cm}^2/\text{V-sec}$ ,  $m^* = 0.25 m$ . Another coating (VDC)<sup>154</sup> formed by hydrolysis at 500–570°C has spectral properties of  $e(100^\circ\text{C}) = 0.15$  and  $T_{\text{solar}} = 0.75$ . The final curves (NF)<sup>119</sup> are for a SnO<sub>2</sub>:Sb coating, which has a resistivity 7.5 ohm/sq.



XBL 809-5967A

Fig. 15. Transmittance of 350 Å of 7.5 percent  $\text{SnO}_2$ /92.5 percent  $\text{In}_2\text{O}_3$  on polymer substrates (PEN-polyethylene naphthalene dicarboxylate, PET-polyethylene terephthalate). PEN is 50 microns and PET, 75 microns thick. Films were prepared by evaporation at 200°C (Teijin).<sup>120</sup> Properties of reactively sputtered  $\text{In}_2\text{O}_3$ :Sn in 10 percent  $\text{O}_2$  are on PET (100mm) are shown for comparison.<sup>63</sup>



XBL 814-5510A

Fig. 16. Two identical 0.3 micron thick  $\text{In}_2\text{O}_3:\text{Sn}$  films except for variation in doping density (atomic percent). Both coatings were prepared by CVD on glass at  $500^\circ\text{C}$  with a reducing atmosphere annealed at  $450^\circ\text{C}$ .<sup>70</sup>

high optical transmission and electrical conductivity.<sup>48</sup> Both magnetron sputtering and CVD are common techniques for the deposition of these films. Specific details of recent research are given in Tables 1A and 1B. For sputtering, cathode targets can be either fused oxide or metal alloys; however, as discussed in Section II, the latter is the least expensive to fabricate.<sup>49</sup> Metal targets must employ a reactive atmosphere for oxide coating. For high quality and conducting films, the degree of oxidation is very important. Optimum conditions can be theoretically calculated.<sup>50</sup> The amount of oxidation may be adjusted by heat treating in air or oxygen atmospheres.<sup>51</sup> From purely an energy savings and production time standpoint, it is not favorable to perform subsequent heat treatments. The effects of an oxygen atmosphere during sputtering and annealing of  $\text{In}_2\text{O}_3$  have been studied in some detail.<sup>52,53</sup> Annealing can act to induce oxygen vacancies and devitrification of the films.<sup>54</sup> The usual property correspondence is that when resistivity is greatest the optical transmission is the highest. But if films were deposited in an oxygen excess atmosphere, further annealing oxidation will only act to increase resistivity. Indium tin oxide can be deposited by RF sputtering on a thermally isolated glass substrate to achieve an annealing effect (lower resistivity and better heat mirror character) during sputtering. By doing so, high substrate temperatures are achieved during deposition. With this technique, the best composition was found to be  $\text{In}_2\text{O}_3$  containing 9 mole percent  $\text{SnO}_2$ .<sup>55</sup>

## SPECTRAL SELECTIVITY OF METAL FILMS

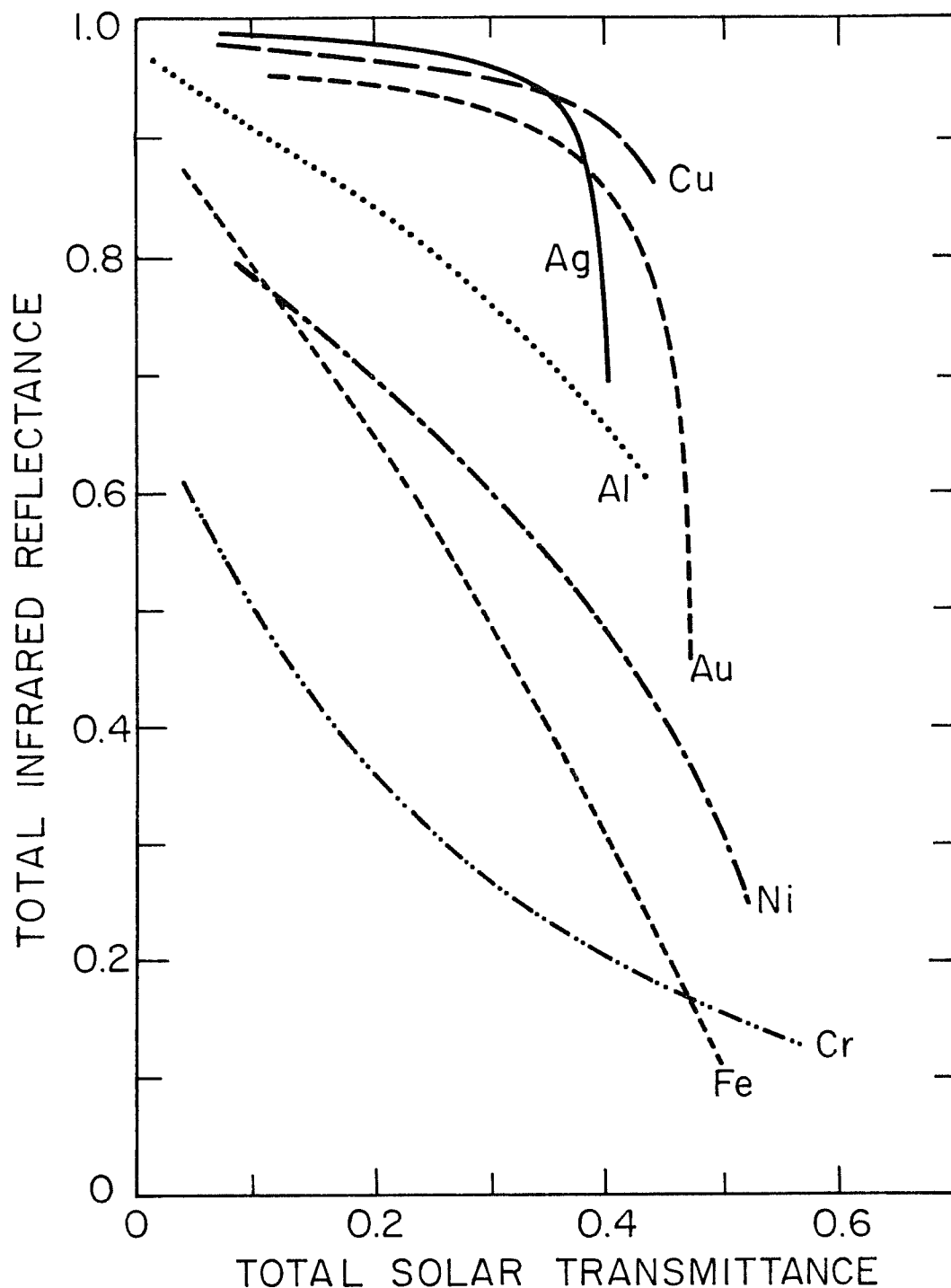


Fig. 18. Integrated infrared reflectance ( $10^{\circ}\text{C}$ ) as a function of transmitted total solar radiation for thin metal films of various thicknesses.<sup>122</sup> For Au, Fe, Cr films thickness ranges from 50–300 Å; Ni and Al films range 25–200 Å, and Ag and Cu films from 95–400 Å.

TABLE 1A. TRANSPARENT CONDUCTIVE OXIDES - SINGLE LAYER MATERIALS - INDIUM TIN OXIDES

Material	Deposition Technique	Sheet Resistance ohm/sq	Thickness Microns	Bulk Resistivity ohm/cm	Mobility cm <sup>2</sup> /V-sec	Carrier Density cm <sup>-3</sup>	Bandgap eV	Ave I <sub>vis</sub>	T <sub>solar</sub>	R <sub>ir</sub> or (E <sub>ir</sub> )	Ref
In <sub>2</sub> O <sub>3</sub>	REACT VAC EVAP 420°C	89	0.045	4 x 10 <sup>-4</sup>	72	4 x 10 <sup>20</sup>	-	-0.6*	-	-	144
In <sub>2</sub> O <sub>3</sub>	REACT VAC EVAP 320-350°C	7.4	0.27	2 x 10 <sup>-4</sup>	70	4 x 10 <sup>20</sup>	3.56, 2.69	<0.9	-	-	175, 159
In <sub>2</sub> O <sub>3</sub>	REACT RF SPUT, DC BIAS	50	0.4	2 x 10 <sup>-3</sup>	25	1.3 x 10 <sup>20</sup>	-	<0.8*	-	-	44
In <sub>2</sub> O <sub>3</sub> : F	CVD	18	1	1.8 x 10 <sup>-3</sup>	-	-	-	-	-	0.75, 7-15µm	124
In <sub>2</sub> O <sub>3</sub> : F	PLAS REACT VAC EVAP 25°C	22	0.1	2.2 x 10 <sup>-4</sup>	8	3.7 x 10 <sup>20</sup>	-	-0.6	-	-	169
In <sub>2</sub> O <sub>3</sub> : F	PLAS REACT VAC EVAP,	17	0.1	1.7 x 10 <sup>-4</sup>	11	3.2 x 10 <sup>21</sup>	-	-0.7	-	-	169
In <sub>2</sub> O <sub>3</sub> : Sn	ANH 450°C	-	-	-	-	-	-	-	0.8-0.9, 0.3-1.5µm	-	125
In <sub>2</sub> O <sub>3</sub> : Sn	SP HYDRO 400-600°C	10	0.5	5 x 10 <sup>-4</sup>	30	5 x 10 <sup>20</sup>	-	-	-	-	84
In <sub>2</sub> O <sub>3</sub> : Sn	SCANNING SP HYDRO 450°C	4	0.5	2 x 10 <sup>-4</sup>	-	-	-	0.92	-	-	126
(Sn/In=0.025)	-	-	-	-	-	-	-	-	-	-	127
In <sub>2</sub> O <sub>3</sub> : Sn(2w/o)	SP HYDRO 400°C	-	-	2 x 10 <sup>-4</sup>	40-50	-	-	0.80	-	-	2
In <sub>2</sub> O <sub>3</sub> : Sn	SP HYDRO	15-20	-	-	-	1.5 x 10 <sup>21</sup>	-	-0.9	-	0.85	157
In <sub>2</sub> O <sub>3</sub> : Sn(3a/o)	SP HYDRO	-	0.15	-	-	-	-	-0.85	<0.8	-	22
In <sub>2</sub> O <sub>3</sub> : Sn	SP HYDRO 400-700°C	135	0.2	2.7 x 10 <sup>-3</sup>	-	-	-	-0.6	-	-	128
In <sub>2</sub> O <sub>3</sub> : Sn	SP PYRO 600-800°C	20 <sup>δ</sup>	-	-	-	5 x 10 <sup>20</sup>	-	0.91, 0.59µm	0.79	0.90, 10µm	-
In <sub>2</sub> O <sub>3</sub> : Sn	SP PYRO 500°C	7-8	0.31	2.2x10 <sup>-4</sup> -2.5x10 <sup>-4</sup>	50	-	-	0.59µm	-	(0.12)	129
In <sub>2</sub> O <sub>3</sub> : Sn(2a/o)	ULTRASONIC SP PYRO 480°C	4	0.6	2.2 x 10 <sup>-4</sup>	-	-	-	0.88	-	-	130
In <sub>2</sub> O <sub>3</sub> : Sn	CVD 450°C	15	0.3	5 x 10 <sup>-3</sup>	5-22	10 <sup>20</sup>	-	0.90+	-	-	65
In <sub>2</sub> O <sub>3</sub> : Sn	CVD 555°C	3	0.75	2.2 x 10 <sup>-4</sup>	-	-	-	0.68	-	-	-

TABLE 1A. Continued

Material	Deposition Technique	Sheet Resistance ohm/sq	Thickness Microns	Bulk Resistivity ohm/cm	Mobility cm <sup>2</sup> /V-sec	Carrier Density cm <sup>-3</sup>	Bandgap eV	Ave T <sub>vis</sub>	T <sub>solar</sub>	R <sub>ir</sub> or (E <sub>ir</sub> )	Ref
In <sub>2</sub> O <sub>3</sub> : Sn (8 a/o)	CVD Organometallic 500-555°C	50	0.165-0.5	4.3x10 <sup>-4</sup> -7.1x10 <sup>-4</sup>	-	-	-	0.83-0.89	-	-	65
In <sub>2</sub> O <sub>3</sub> : Sn**	VAC EVAP 200°C, ANN 180-200°C	200-500	0.02-0.05	1x10 <sup>-3</sup> -3x10 <sup>-3</sup>	10	3 x 10 <sup>20</sup> - 4 x 10 <sup>20</sup>	-	0.80-0.95	-	-	120
In <sub>2</sub> O <sub>3</sub> : Sn	REACT VAC EVAP 400°C	40-60	0.08	5 x 10 <sup>-3</sup>	-	-	-	0.80	-	-	131
In <sub>2</sub> O <sub>3</sub> : Sn	REACT VAC EVAP 400°C	~8	~0.25	2 x 10 <sup>-4</sup>	30	1 x 10 <sup>21</sup>	4.1	~0.8*	-	0.8, 6μm	144
In <sub>2</sub> O <sub>3</sub> : Sn	VAC EVAP 0-200°C,	-	-	2 x 10 <sup>-3</sup>	10	2 x 10 <sup>20</sup>	-	-	-	-	80
In <sub>2</sub> O <sub>3</sub> : Sn	ANN AIR 300-500°C	187	0.08	1.5 x 10 <sup>-3</sup>	-	-	-	~0.6	-	-	32
In <sub>2</sub> O <sub>3</sub> : Sn	PLAS REACT VAC EVAP RT	25	0.4	1 x 10 <sup>-3</sup>	-	-	-	-	0.96, 0.4-1.6μm	-	146
In <sub>2</sub> O <sub>3</sub> : Sn	PLAS REACT VAC EVAP 350°C	2.2	1	2.2 x 10 <sup>-4</sup>	-	-	-	-	0.88, 0.4-1.6μm	-	146
In <sub>2</sub> O <sub>3</sub> : Sn	PLAS REACT VAC EVAP 350°C	-	-	7 x 10 <sup>-4</sup>	20-30	10 <sup>21</sup>	-	-	>0.9, 0.4-1.2μm	-	148
In <sub>2</sub> O <sub>3</sub> : Sn	PLAS REACT VAC EVAP 370°C	2-3	0.9-0.6	1.77 x 10 <sup>-4</sup>	-	-	-	0.80	-	0.9, 2.5-15μm	133
In <sub>2</sub> O <sub>3</sub> : Sn (9 m/o)	DC SPUT in Ar 500°C	100	0.15	1.5 x 10 <sup>-3</sup>	-	-	-	0.85	-	-	134
In <sub>2</sub> O <sub>3</sub> : Sn	REACT DC SPUT, ANN 525°C	<40	0.55	<2.2 x 10 <sup>-3</sup>	-	-	-	>0.9*	-	-	147
In <sub>2</sub> O <sub>3</sub> : Sn	REACT DC SPUT, ANN 300-500°C	-	-	1 x 10 <sup>-4</sup>	-	-	3.7, 2.6	-	-	-	59
In <sub>2</sub> O <sub>3</sub> : Sn	RF SPUT	6	0.35	1.1 x 10 <sup>-3</sup>	-	-	-	-	0.85 <sup>a</sup> (4M2)	(0.081, 121°C)	71, 135
In <sub>2</sub> O <sub>3</sub> : Sn	RF SPUT in Ar 600°C	-	0.35	-	-	-	-	-	0.90 <sup>a</sup> (4M2)	(0.081, 121°C)	71, 135
In <sub>2</sub> O <sub>3</sub> : Sn/ 1000Å MgF <sub>2</sub>	RF SPUT in Ar 600°C	25	0.25	6.25 x 10 <sup>-4</sup>	-	-	-	0.93	-	-	69
In <sub>2</sub> O <sub>3</sub> : Sn	RF SPUT in Ar	2-3	-	-	-	-	-	0.80	-	-	87
In <sub>2</sub> O <sub>3</sub> : Sn	RF SPUT in Ar 400°C	-	-	-	-	-	-	-	-	-	-

TABLE 1A. Continued

Material	Deposition Technique	Sheet Resistance ohm/sq	Thickness microns	Bulk Resistivity ohm/cm	Mobility cm <sup>2</sup> /V-sec	Carrier Density cm <sup>-3</sup>	Bandgap eV	Ave I <sub>vis</sub>	T <sub>solar</sub>	R <sub>ir</sub> or (E <sub>ir</sub> )	Ref
In <sub>2</sub> O <sub>3</sub> :Sn**	RF SPUT in O <sub>2</sub> 40-180°C	62.5	0.08	5 x 10 <sup>-4</sup>	10	10 <sup>21</sup>	-	>0.85, 0.4-0.8μm	-	-	30
In <sub>2</sub> O <sub>3</sub> : Sn	RF SPUT in Ar 550°C	2.6	<0.3	-1 x 10 <sup>-4</sup>	38	7 x 10 <sup>20</sup>	-	>0.8*	-0.8*	0.92, 10μm	55
In <sub>2</sub> O <sub>3</sub> : Sn	RF SPUT in Ar 600°C, etched Microgrid	3	0.35	1 x 10 <sup>-4</sup>	-	-	-	-	0.90(AM2)	0.83, 10μm	135
In <sub>2</sub> O <sub>3</sub> : Sn	RF SPUT, etched Microgrid	6 <sup>a</sup>	0.35	2 x 10 <sup>-4</sup>	-	-	-	-	0.9	0.83	73
In <sub>2</sub> O <sub>3</sub> : Sn	RF SPUT Ar, ANN	-	-	1.2 x 10 <sup>-2</sup>	-	-	3.05	-	-	-	58
In <sub>2</sub> O <sub>3</sub> : Sn	RF SPUT Ar, ANN H <sub>2</sub> 400°C	5.5	1.5	8.3 x 10 <sup>-4</sup>	-	-	3.42	0.90	-	-	58
In <sub>2</sub> O <sub>3</sub> : Sn	RF SPUT O <sub>2</sub> , ANN Ar 600°C	2-3	-	-	-	-	-	0.95	-	-	48
In <sub>2</sub> O <sub>3</sub> : Sn	CYL SPUT O <sub>2</sub> 20-400°C, ANN 400°C	-	0.3-1.5	2 x 10 <sup>-4</sup> -5x10 <sup>-4</sup>	30	6 x 10 <sup>20</sup>	-	0.8-0.9*	-	-	61
In <sub>2</sub> O <sub>3</sub> : Sn	REACT RF SPUT O <sub>2</sub> -Ar 400°C	10	0.31	3 x 10 <sup>-4</sup>	40	5 x 10 <sup>20</sup>	-	-0.8	-	-0.82	136
In <sub>2</sub> O <sub>3</sub> : Sn	REACT RF SPUT O <sub>2</sub> -Ar 450°C	-6-4	0.5-0.8	-3 x 10 <sup>-4</sup>	-35	-6 x 10 <sup>20</sup>	-	-0.9, 0.45-0.8μm	-	-	138
In <sub>2</sub> O <sub>3</sub> :Sn**	REACT RF SPUT O <sub>2</sub> -Ar 140-180°C,	<30	0.5	2.5 x 10 <sup>-3</sup>	-	-	-	0.8*, 0.55μm	-	-	63
In <sub>2</sub> O <sub>3</sub> : Sn	REACT RF SPUT O <sub>2</sub> -Ar 260°C, PH 100°C	50	0.5	2.5 x 10 <sup>-3</sup>	-	-	-	0.94	-	-	49
In <sub>2</sub> O <sub>3</sub> : Sn	REACT RF SPUT O <sub>2</sub> -Ar, PH 375°C	100	0.03	3 x 10 <sup>-4</sup>	-	-	-	0.97	-	-	49
In <sub>2</sub> O <sub>3</sub> : Sn	REACT RF SPUT O <sub>2</sub> -Ar, ANN H <sub>2</sub> -H <sub>2</sub>	150-200	-	-	-	-	-	0.90-0.95	-	-	139

TABLE IA. Continued

Material	Deposition Technique	Sheet Resistance ohm/sq	Thickness Microns	Bulk Resistivity ohm/cm	Mobility cm <sup>2</sup> /V-sec	Carrier Density cm <sup>-3</sup>	Bandgap eV	Ave T <sub>vis</sub>	T <sub>solar</sub>	R <sub>ir</sub> or {E <sub>ir</sub> }	Ref
In <sub>2</sub> O <sub>3</sub> : Sn	REACT RF SPUT O <sub>2</sub> 400°C, ANN 600°C	3	0.4	$-1.2 \times 10^{-4}$	50	10 <sup>21</sup>	-	-	-	-0.9	136
In <sub>2</sub> O <sub>3</sub> : Sn**	REACT IB SPUT O <sub>2</sub> 80°C	11-9	0.5-0.6	$5.5 \times 10^{-4}$	50	$4 \times 10^{20}$	-	>0.9	-	0.84, 10 $\mu$ m	35
In <sub>2</sub> O <sub>3</sub> : Sn	PLAS REACT SPUT Ar-O <sub>2</sub> RT	-	-	$2 \times 10^{-4}$	10	$3 \times 10^{20}$	-	0.7-0.8*	-	>0.9	31
In <sub>2</sub> O <sub>3</sub> : Sn	PLAS REACT SPUT RT	250	0.10	$2.5 \times 10^{-3}$	9	$3 \times 10^{20}$	-	0.7-0.8*	-	-	31,33
In <sub>2</sub> O <sub>3</sub> : Sn	PLAS REACT SPUT RT	<30	0.33	$<1 \times 10^{-3}$	20	$5 \times 10^{20}$	-	0.75, 0.55 $\mu$ m*	-	0.75, 4 $\mu$ m*	64

\* Includes substrate

\*\* On polymer substrate, or can be used on one

a T<sub>glass</sub> = 0.906

2a) Before etching

6 A range of  $10^{-10}^5$  has been reported



TABLE 1B. Continued

Material	Deposition Technique	Sheet Resistance ohm/sq	Thickness Microns	Bulk Resistivity ohm/cm	Mobility cm <sup>2</sup> /V-sec	Carrier Density cm <sup>-3</sup>	Bandgap eV	Ave $\tau_{vis}$	T <sub>solar</sub>	R <sub>ir</sub> or (E <sub>ir</sub> )	Ref
SnO <sub>2</sub> :Sb (2 m/o)	SP HYDRO 570-620°C	8.6	0.78	6.7 x 10 <sup>-4</sup>	17	5.6 x 10 <sup>20</sup>	-	-	-0.7	(0.19)	154
SnO <sub>2</sub> :Sb	SP HYDRO 500-725°C	~150	-	-	-	-	-	-0.85	-	-	67
SnO <sub>2</sub> :Sb	SP HYDRO 600-680°C	62	-	-	-	-	-	-0.9	-	-	22
SnO <sub>2</sub> :Sb	CVD 500-630°C	-	-	3.2 x 10 <sup>-3</sup>	-	-	-	0.4-0.72 μm	-	-	85,86
SnO <sub>2</sub> :Sb	CVD Organometallic, 400-550°C	50-150	0.15-0.36	4x10 <sup>-4</sup> -1.1x10 <sup>-4</sup>	18-35	2x10 <sup>19</sup> -5x10 <sup>20</sup>	-	-	-	-	15,149
SnO <sub>2</sub> :Sb (0.6-2.7a/o)	CVD CONV. FURN 500°C	140	0.1	1.5x10 <sup>-3</sup>	23	1.2 x 10 <sup>20</sup>	-	0.85-0.91	-	-	23
SnO <sub>2</sub> :Sb	CVD CONV. FURN 500°C	1400	0.01	1.5 x 10 <sup>-3</sup>	-	-	-	0.9, 0.55 μm*	-	-	23
SnO <sub>2</sub> :Sb	CVD CONV. FURN 500°C	70	0.1	7 x 10 <sup>-4</sup>	-	-	-	0.92, 0.55 μm*	-	-	23
SnO <sub>2</sub> :Sb <sup>δ</sup>	CVD CONV. FURN 500°C	700	0.01	7 x 10 <sup>-4</sup>	-	-	-	0.9, 0.55 μm*	-	-	23
SnO <sub>2</sub> :Sb	REACT DC SPUT, ANN 710°C	175	0.35	6.1 x 10 <sup>-3</sup>	-	-	-	0.92, 0.55 μm*	-	-	54

NOTE: All compounds designated SnO<sub>2</sub> may or may not be doped

\* includes substrate

a can be used on polyester

δ on SiO<sub>2</sub>

\*\* Moving substrate 0-15 M/min

The chemical properties of  $\text{In}_2\text{O}_3$  films have been evaluated.<sup>56</sup> In films with good optical and electrical properties, a Sn-rich surface was noted. The study revealed that film darkening was caused by the nucleation and growth of a secondary phase similar to  $\text{Sn}_3\text{O}_4$  in composition. Many annealed films exhibit a brownish cast.<sup>48</sup> In the bulk, the  $\text{Sn}_3\text{O}_4$  phase can be suppressed by using higher substrate temperatures to bring close chemical equilibrium during RF sputtering. Also, microstructural data is known for RF sputtered ITO and  $\text{SnO}_2$ .<sup>57</sup>

During sputtering of  $\text{In}_2\text{O}_3\text{:Sn}$  films, dendritic precipitates (60 microns long) have been noted to form under adverse conditions. Their presence has been correlated to decreased visible transmittance by optical scattering.<sup>58</sup> Highly conducting films have been obtained with metal excess compositions (shown in Fig. 16). Annealing and reducing agents such as 2 percent pyrogallol solution have been used to make substoichiometric films.<sup>22</sup> In highly conductive films, the optical absorption edge is noted to shift when the carrier concentration changes from  $10^{19}$  to  $8.2 \times 10^{20} \text{ cm}^{-3}$ . From the optical properties of  $\text{In}_2\text{O}_3\text{:Sn}$  it was also found that  $m^* = 0.43 m$  at high carrier concentrations.<sup>59</sup>

The optimum composition of sputtered ITO films has been given by one author<sup>60</sup> as  $\text{In}_{1.9}\text{Sn}_{0.1}\text{O}_3$ . At a thickness of 0.24 microns these films have  $T_{\text{vis}} = 0.85$ . These films exhibit a BCC structure with 1000 Å wide fibrous grains. The best deposition temperatures are between 500–700°C with rates up to 0.3 microns per minute.<sup>60</sup>

Oxygen pressure during RF reactive sputtering has a great effect on the ultimate optimization of  $\text{In}_2\text{O}_3\text{:Sn}$  films. A narrow range of optimum pressures from  $3 \times 10^{-5}$  –  $4 \times 10^{-5}$  torr give films of  $3 \times 10^{-4}$  ohm-cm and  $T_{\text{vis}} = 0.9$ . The plasma edge can be adjusted by the Sn doping in  $\text{In}_2\text{O}_3$ .

A relationship between sputtering power and oxygen pressure has been devised for reactive sputtering of ITO.<sup>50</sup> The best optical and electrical properties occur near but below the critical concentration of  $\text{O}_2$ . Below the critical concentration film stoichiometry begins to deviate. These are conditions where 100 percent oxygen is insufficient to oxidize indium.<sup>50</sup>

Cylindrical magnetron sputtering has been successfully used with ITO.<sup>61</sup> Thick films of ITO greater than 1 micron have had loss of adherence during deposition. Compressive stresses of  $\sigma = -1.81 \times 10^{10}$  dyns  $\text{cm}^{-2}$  have been noted, not dependent upon film thickness. Annealing reduced these stresses to less than half.<sup>62</sup>

High-rate magnetron sputtering has recently been performed on polyester (PET) film in a roll coating apparatus. Deposition rates of 200–4500 Å/min have been achieved using a water-cooled substrate.<sup>63</sup> A relationship between resistivity and reflectivity has also been noted. Examples of these films are shown in Fig. 15. RF ion plating with a DC magnetron source at near room temperature<sup>64</sup> has yielded deposition rates of 500 Å/min for films of  $\text{In}_2\text{O}_3\text{:Sn}$  with resistivity of about  $1 \times 10^{-3}$  V-cm and mobility of  $20 \text{ cm}^2 \text{ V}^{-1} \text{ sec}^{-1}$ . Electron beam evaporation can give 3600 Å/min rates for 0.9  $\text{In}_2\text{O}_3$ /0.1  $\text{SnO}_2$ .

Films of  $\text{In}_2\text{O}_3:\text{Sn}$  have been deposited by CVD using organometallic reagents at  $500^\circ\text{C}$ . The best films produced by this technique have visible transmission above 0.89 and resistivity of  $4.3 \times 10^{-4}$  ohm-cm.<sup>65</sup> A wide variation of index of refraction has been noted also (1.67–2.48).<sup>65</sup> The intrinsic band gap of  $\text{In}_2\text{O}_3$  is 3.55 eV with an indirect forbidden 2.4 eV transition.<sup>66</sup> For ITO films deposited by CVD below  $400^\circ\text{C}$ , an amorphous structure is noted.<sup>67</sup> Generally, ITO films formed at higher temperatures consist of polycrystalline  $\text{In}_2\text{O}_3$  in a BCC structure with [111] or [100] preferred perpendicular orientation with respect to the substrate.<sup>68,69</sup> Undoped  $\text{In}_2\text{O}_3$  films can be prepared by thermal evaporation at  $320\text{--}350^\circ\text{C}$  of In,  $\text{In}_2\text{O}_3$ , with  $2 \times 10^{-4}$  ohm-cm and  $T_{\text{vis}} > 0.9$ ; values that rival ITO. The plasma edge can be adjusted by the Sn doping in  $\text{In}_2\text{O}_3$ . One experiment<sup>70</sup> showed for 2 percent Sn,  $N = 0.5 \times 10^{21} \text{ cm}^{-3}$  and  $w_p = 1.6 \text{ } \mu\text{m}$  compared to 8 percent Sn,  $N = 1.3 \times 10^{21} \text{ cm}^{-3}$  and  $w_p = 1.1 \text{ } \mu\text{m}$ . These results are shown in Fig. 16. The relationships between sheet resistance, mobility carrier concentration, and IR emittance are known for CVD-prepared ITO.

Further visible and solar transmittance gains can be made by the addition of a second-layer antireflection coating, such as 100 Å of  $\text{MgF}_2$ .<sup>71</sup> Another gain can be achieved by selectively etching a grid pattern in the oxide surface using photolithographic techniques. A regular array of 2–3 micron openings would behave as an electromagnetic radiation filler, allowing solar energy to pass through and infrared

energy to be reflected.<sup>72</sup> Solar transmission can be improved from 0.8 to 0.9 while reducing IR reflectance 0.91 to 0.83 for ITO films.<sup>73</sup>

#### B. Transparent Conductive Oxides: Tin Oxide

Doped tin oxide films are very similar to ITO films. The various PVD and CVD deposition techniques are applicable to both systems. Generally, dopants for the  $\text{SnO}_2$  system consist of antimony, fluorine, and phosphorus. The key to optimum doping is that all dopant atoms occupy electrically active sites and have fairly compatible energy levels with the host lattice. The common doping levels for antimony and phosphorus are within about 1–3 mole percent. Fluorine gives about two times the electron mobility ( $40 \text{ cm}^2/\text{V-sec}$ ) of the other dopants in  $\text{SnO}_2$ , at much higher doping levels. This difference is caused by the existence of a higher electron mean-free path due to decreased scattering between energy levels in  $\text{SnO}_2:\text{F}$ . At temperatures above  $200^\circ\text{C}$  thermal aging is noticed in  $\text{SnO}_2:\text{F}$ , particularly in vacuum of high temperature solar collectors.<sup>74</sup> The net effect is probably reduction of  $\text{SnO}_2$ , resulting in decreased mobility and increased emittance. Soviet work on doped  $\text{SnO}_2$  for solar transparent insulation was reviewed some time ago.<sup>75</sup>

The lowest resistivity  $\text{SnO}_2:\text{Sb}$  films lie within the region of 0.015–0.030 gram Sb per gram Sn. Although the deposition conditions do heavily dictate the final film properties, the physical, electrical, and optical properties of intrinsic and doped single-crystal  $\text{SnO}_2$  have been

reviewed by Jarzebski.<sup>76-78</sup> The structure and growth mechanisms of CVD sprayed  $\text{SnO}_2\text{:Sb}$  films have been studied.<sup>79</sup>

Tin oxide films can also be made by vacuum deposition of the metallic tin or suboxides<sup>80</sup> followed by an oxygen heat treatment at  $500^\circ\text{C}$ .<sup>81</sup> A new technique for  $\text{SnO}_2$  deposition has recently been devised which incorporates a CVD process between a float glass furnace and annealing lehr. High velocity reactive gases are blown onto the hot glass surface in this technique. Substrate velocities of 8-15 m/min have been achieved with quality coatings 5 ohm/sq at 0.6 microns thick. This method can also be used for  $\text{TiO}_2$ .<sup>82</sup> A potentially large-scale CVD organometallic process is also being developed for glass substrates without annealing.<sup>27</sup> Another batch CVD process for  $\text{SnO}_2\text{:Sb}$  using large industrial furnaces has yielded  $10^{-3}$  ohm-cm coatings of 500-3000 Å with  $\pm 10$  percent thickness control; such properties are suitable for electronic displays.<sup>83</sup> Yet another CVD hydrolysis process uses a scanning nozzle to cover large areas.<sup>84</sup>

In CVD-fabricated  $\text{SnO}_2\text{:Sb}$  polycrystalline films, only  $\text{SnO}_2$  has been detected by chemical analysis.<sup>85,86</sup>  $\text{SnO}_2$  is found in the form of agglomerated crystallites with (200), (301) atomic planes oriented parallel to the film surface. The decrease in mobility with doping is assumed to be directly related to impurity scattering effects. In films of  $\text{SnO}_2\text{:F}$  deposited by CVD at  $500^\circ\text{C}$ , both polycrystalline phases of  $\text{SnO}_2$  and  $\text{SnO}$  were detected,<sup>87,88</sup> and should be detected in most films.

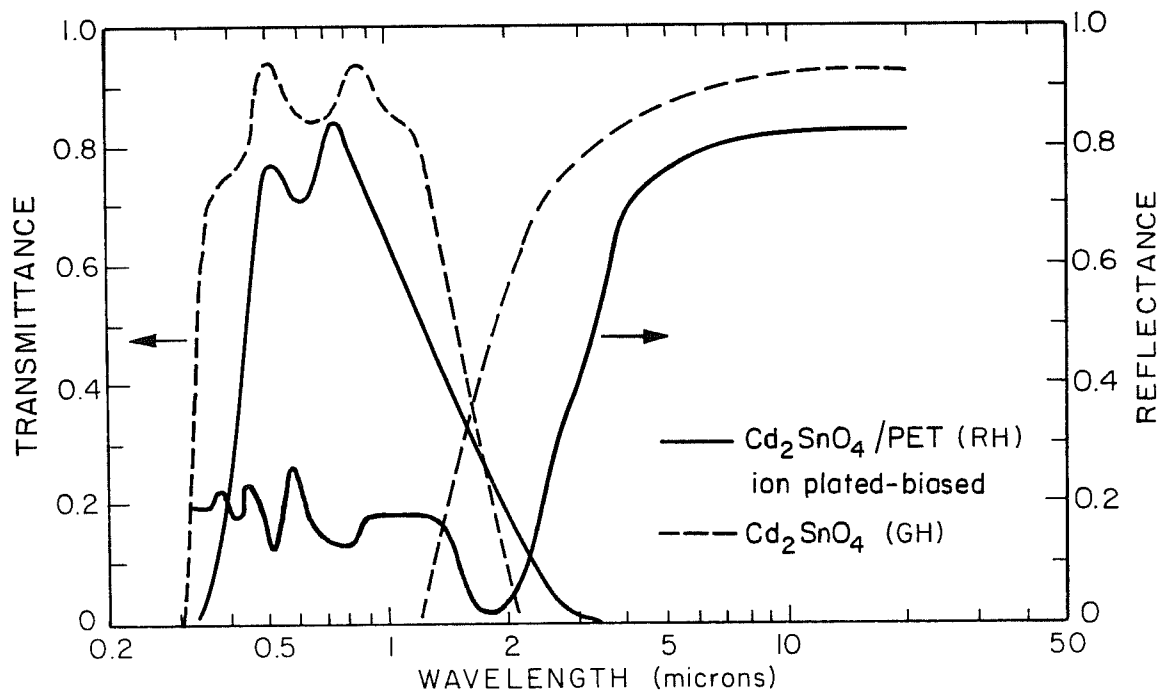
The defect structure of pure  $\text{SnO}_2$  appears to be either the result of doubly ionized oxygen vacancies or interstitial ions.<sup>76</sup> The structure of pure  $\text{SnO}_2$  is tetragonal. Anion deficiency in pure  $\text{SnO}_2$  causes lattice distortion which permits electrons to occupy the normally forbidden energy bands, thereby producing extrinsic semiconductivity.<sup>88</sup>

The doping effects of Sb, P, Tl, and In in pyrolytic films of (casiterite structure)  $\text{SnO}_2$  have been studied.<sup>89</sup> Trivalent Tl and In act to increase resistivity while Sb and P decrease it. The effect of doping and pentavalent oxygen vacancies both favor the formation of  $\text{Sn}^{+4} \rightarrow \text{Sn}^{+2}$ . By pentavalent doping the intrinsic donor level at 0.0175 eV from the conduction band can be reduced as low as 0.0015 eV, forming a donor band. This decrease in activation energy increases conduction. Also, with trivalent addition IR transmission decreased and pentavalent species acted to increase it. Large concentrations of Sb dopant can result in an amorphous  $\text{SnO}_2:\text{Sb}$  that is highly resistive.<sup>90</sup> The doping of  $\text{SnO}_2$  with boron ( $\text{H}_3\text{BO}_3$ ) has been studied<sup>76</sup> along with growth and film structure for  $\text{SnO}_2:\text{Sb}$ .<sup>44</sup> Also, the structure of  $\text{SnO}_x$  films has been studied.<sup>91</sup> For oxygen concentration ranging from 10–15 percent in  $\text{SnO}_x$ , conductivity is the lowest. The structure of the conducting film is  $\text{SnO}_2$  with some  $\alpha\text{-SnO}$ . Below this concentration to 4 percent oxygen,  $\alpha\text{-SnO}_2$ ,  $\text{SnO}_2$ , and  $\beta\text{-Sn}$  coexist. Below 4 percent oxygen concentration,  $\beta\text{-Sn}$  and  $\alpha\text{-SnO}$  coexist.<sup>91</sup>

### C. Transparent conductive oxides: Cadmium Stannate

Another favored transparent conductor is cadmium stannate,  $\text{Cd}_2\text{SnO}_4$ ; it shows good durability and chemical resistance. By increasing film conductivity, transparency is improved, which is contrary to expectations (see Fig. 17). The reason for this is due to its large Burstein shift and high electron mobility. The Burstein shift is essentially an absorption edge shift to lower wavelengths after conduction band saturation. The effect occurs in semiconductors with low effective mass (for  $\text{Cd}_2\text{SnO}_4$ ,  $m^* \sim 0.04 m$ ) indicating high conduction band curvature. The density of states at the bottom of the conduction band is low, and those states can fill up at relatively small free carrier concentrations, forcing the fundamental optical absorption edge to higher energies. The limit to the increased transparency in  $\text{Cd}_2\text{SnO}_4$  is achieved when the free carrier concentration exhibits its dominant plasma absorption as the material becomes degenerate.

Films with resistivity ranging from 1-100 ohm/sq have been fabricated.<sup>92</sup> These films are n-type with oxygen vacancies, which provide donor states in the bandgap.<sup>93</sup> Both crystalline and amorphous phases have been prepared, as outlined in Table 1c. Recently, ion plating  $\text{Cd}_2\text{SnO}_4$  has been deposited on polyester substrates<sup>19</sup>; its optical properties are shown in Fig. 17. Films of  $\text{Cd}_2\text{Sn}$  can be made near room temperature at rates of 500 Å/min by ion plating.<sup>64</sup> Films with resistivities of  $1 \times 10^{-3}$  ohm/cm and mobilities of  $35 \text{ cm}^2/\text{V-sec}$  are possible.



XBL 815 -5506A

Fig. 17. Two  $\text{Cd}_2\text{SnO}_4$  coatings. One is (RH)<sup>19</sup> produced by ion plating on a polyester substrate. It is annealed with film properties of  $t = 0.32$  microns and  $R = 6 \times 10^{-4}$  ohm-cm. The second (GH)<sup>121</sup> is RF sputtered on glass with an annealing step.

Amorphous films are made by RF sputtering from a polycrystalline  $\text{Cd}_2\text{SnO}_4$  target. Both the electrical and optical properties of the film can be altered by annealing. High conductivity films are achieved by sputtering in argon or by subsequent annealing at 200–300°C for 2–30 minutes in a reducing atmosphere.<sup>93</sup> The bandgap of  $\text{Cd}_2\text{SnO}_4$  has been estimated as 2.06 eV, but can shift to 2.85 eV. Cadmium stannate film has a critical thickness of 0.3 microns, below which the infrared reflectance declines.<sup>94</sup> The substrate temperature is very important to the properties of the film. Lesser properties are obtained at near room temperature.

Crystalline films of lower resistivity have been made by RF sputtering at  $6 \times 10^{-3}$  torr onto glass<sup>94</sup>; however, their conductivities were low  $\sim 10 \text{ ohm}^{-1} \text{ cm}^{-1}$ . A postdeposition treatment in Argon/CdS atmosphere at temperatures ranging from 600°C to 700°C shifts the absorption edge from 2 to 2.9 eV. The best films were sputtered in pure oxygen at 500°C at 600 watts, 13.6 MHz RF power. Films ranging from 1.2 ohm/sq to 3.4 ohm/sq were made for deposition times of 1.3 hr to 0.4 hr, respectively. All films were annealed after deposition for 10 min at 690°C in Ar/CdS atmosphere.<sup>94</sup>

In  $\text{Cd}_2\text{SnO}_4$  there is difficulty in keeping the secondary phases  $\text{CdSnO}_3$  and  $\text{CdO}$  out of the films.<sup>95</sup> It has been shown that  $\text{CdSnO}_3$  as a pure film is also a good transparent conductor, as shown in Table 1C. However,  $\text{Cd}_2\text{SnO}_4$  has slightly better optical properties. High quality film can be deposited from CdSn alloy targets in an oxygen plasma if Cd ratio is kept 2 Cd:Sn.<sup>95</sup> This means a less expensive

TABLE 1C. TRANSPARENT CONDUCTIVE OXIDES - SINGLE LAYER MATERIALS - CADMIUM TIN OXIDES

Material	Deposition Technique	Sheet Resistance ohm/sq	Thickness Microns	Bulk Resistivity ohm/cm	Mobility cm <sup>2</sup> /V-sec	Carrier Density cm <sup>-3</sup>	Bandgap eV	Ave T <sub>lys</sub>	T <sub>solar</sub>	R <sub>ir</sub> or (E <sub>ir</sub> )	Ref
CdSnO <sub>3</sub>	RF SPUT	-	-	1 x 10 <sup>-3</sup>	-	-	>3	-	-	-	94
CdSnO <sub>3</sub>	SP PYRO <800°C	10-20	-	-	-	-	-	-0.7*	-	-	150
α-Cd <sub>2</sub> SnO <sub>4</sub>	RF SPUT in Ar	76	0.34	2.6 x 10 <sup>-3</sup>	20	1 x 10 <sup>20</sup>	2.85	-	-	-	93
α-Cd <sub>2</sub> SnO <sub>4</sub>	REACT RF SPUT in Ar-O <sub>2</sub> , ANN H <sub>2</sub>	2.3	3.3	7.5 x 10 <sup>-4</sup>	-	-	>3	-	-	-	94
α-Cd <sub>2</sub> SnO <sub>4</sub>	RF SPUT <100°C, ANN 670°C	>10	-	-	-	-	-	0.85, 0.5-0.65μm	-	-	94
Cd <sub>2</sub> SnO <sub>4</sub>	SP PYRO, ANN 300°C	-	-	-	-	-	2.8, 2.2	0.82	-	(0.09)	92
Cd <sub>2</sub> SnO <sub>4</sub>	SP PYRO, >800°C, ANN 850°C	80-100	-	-	1-5	-	-	0.85-0.9	-	-	150
Cd <sub>2</sub> SnO <sub>4</sub>	RF SPUT	-	<0.3	-	-	-	-	-	0.89	(0.2, 77°C)	121
Cd <sub>2</sub> SnO <sub>4</sub>	RF SPUT in Ar 200°C	-	0.15-0.25	6.5 x 10 <sup>-4</sup>	-	-10 <sup>19</sup>	2.23	-0.9	-	-	151
Cd <sub>2</sub> SnO <sub>4</sub>	RF SPUT, ANN 420°C	-26-43	<0.3	-	-	-	-	-	0.86	(0.12, 77°C)	121
Cd <sub>2</sub> SnO <sub>4</sub>	RF SPUT in Ar 200°C	-	-	2 x 10 <sup>-4</sup>	-	-10 <sup>21</sup>	2.53	-	-	-	151
Cd <sub>2</sub> SnO <sub>4</sub>	ANN 500°C	-	-	-	-	-	-	-	-	-	-
Cd <sub>2</sub> SnO <sub>4</sub>	RF SPUT, ANN 400°C	5	-1	-5 x 10 <sup>-4</sup>	35	4x10 <sup>18</sup> -5x10 <sup>20</sup>	-	>0.7*, 0.55μm	-	-	152

target can be used; in the past, targets were made from sintered powders of exactly  $\text{Cd}_2\text{SnO}_4$ . During RF sputtering, if the substrate is below  $700^\circ\text{C}$  then principally amorphous films result; above that they are mainly crystalline, as determined by X-ray diffraction.<sup>95</sup>

Transparent films of  $\text{Cd}_2\text{SnO}_4$  have been prepared without annealing by DC reactive sputtering in  $\text{Ar-O}_2$  from a  $\text{Cd}_2\text{Sn}$  alloy.<sup>96</sup> The oxygen defect density is adjusted by controlling the oxidation rate at the substrate. This is accomplished by an RF bias on the target and a physical slitting arrangement. Values of  $R = 4.4 \times 10^{-4}$  ohm-cm with transparency of  $T_{\text{vis}} = 0.85$  for 0.15 micron thick films. A deposition rate of 0.015 microns/min was used.

The chemical stability of  $\text{Cd}_2\text{SnO}_4$  is very good. Cadmium stannate films have been used as electrodes in photogalvanic cells and can withstand contact with sulfuric acid electrolyte.<sup>97</sup>

#### D. Transparent conductive oxides: Miscellaneous systems

Various conductive materials exist which have had singular or limited application; however, they are of importance because they may offer a viable heat mirror material. These compounds are tabulated in Table 1D.

One such system,  $\text{CdS}_x\text{:In}$ , developed for photovoltaics appears to have some promise as a heat mirror since it has high visible transparency with low resistivity and high electron mobility. The infrared properties need to be examined. Alloys of  $\text{Cd}_{1-x}\text{Zn}_x\text{S}$  appear interesting, also.<sup>98</sup> Soviet investigators have used antimony-lead

TABLE 10. TRANSPARENT CONDUCTIVE COATINGS - SINGLE LAYER MATERIALS - MISCELLANEOUS COMPOUNDS

Material	Deposition Technique	Sheet Resistance ohm/sq	Thickness Microns	Bulk Resistivity ohm/cm	Mobility cm <sup>2</sup> /V-sec	Carrier Density cm <sup>-3</sup>	Bandgap eV	Ave T <sub>vis</sub>	T <sub>solar</sub>	R <sub>ir</sub> or (E <sub>ir</sub> )	Ref
Bi <sub>2</sub> O <sub>3</sub>	SPUT	-	0.12	-	-	-	-	0.78, 0.56μm	-	(0.34)	116
Bi <sub>2</sub> O <sub>3</sub>	SPUT, ANN 300°C	-	0.12	-	-	-	-	0.825, 0.56μm	-	(0.325, 0.4-2μm)	116
CdO	REACT SPUT N <sub>2</sub> -O <sub>2</sub> , ANN 100°C	26	0.17	4.5 x 10 <sup>-4</sup>	120	1.2 x 10 <sup>20</sup>	-	0.59, 0.6μm	-	-	137
CdO	REACT SPUT N <sub>2</sub> -O <sub>2</sub> 240°C	29	0.13	3.7 x 10 <sup>-4</sup>	120	1.4 x 10 <sup>20</sup>	-	0.71, 0.6μm	-	-	137
CdO	REACT SPUT N <sub>2</sub> -O <sub>2</sub> , ANN 340, 400°C	82	0.18	1.45 x 10 <sup>-3</sup>	120	3.6 x 10 <sup>19</sup>	-	0.74, 0.6μm	-	-	137
CdO	REACT SPUT Ar-O <sub>2</sub>	88	0.243	2.1 x 10 <sup>-3</sup>	7.9	10 <sup>20</sup>	2.5	0.80, 0.65μm	-	-	156
CdO:In(5a/o)	REACT SPUT Ar-O <sub>2</sub>	188	0.281	5.3 x 10 <sup>-3</sup>	2.3	-	-2.5	0.80, 0.65μm	-	-	156
CdO:Cu(5a/o)	REACT SPUT Ar-O <sub>2</sub>	390	0.243	9.4 x 10 <sup>-3</sup>	3.2	-	-2.5	0.65, 0.65μm	-	-	156
CdS <sub>x</sub> :In(1.5a/o)	VAC EVAP 250°C	-	3-4	1x10 <sup>-3</sup> -6x10 <sup>-3</sup>	50-90	-	-	0.9-0.65	-	-	158
Cu <sub>2</sub> S	VAC EVAP	70	-	-	-	-	-	0.48	-	0.6, 10μm	115
Cu <sub>2</sub> S <sub>1.89-1.95</sub>	VAC EVAP 50°C	333-1515	0.13-0.6	9x10 <sup>-3</sup> -5x10 <sup>-1</sup>	-	-	1.85-2.16	0.1-0.7, 0.7μm	-	-	161
Cu <sub>2</sub> S <sub>x</sub>	VAC EVAP 80°C	-	-	-	-	-	-	-	0.37	0.74, 10μm	162
Cu <sub>2</sub> S <sub>1+x</sub>	VAC EVAP, ANN 80°C in S	15	0.65	9.75 x 10 <sup>-4</sup>	-	-	-	0.3-0.35, 0.65μm	-	0.8-0.85, 5μm	100
Cu <sub>2</sub> S <sub>1+x</sub>	VAC EVAP, ANN 80°C in S	44	-	-	-	-	-	0.5, 0.65μm	-	0.8, 8μm	100
Cu <sub>3</sub> SeO <sub>x</sub>	VAC EVAP	-	-	-	-	-	-	-	0.45	0.68, 10μm	162
La <sub>0.6</sub>	EB VAC EVAP 1000°C <sup>3</sup>	2	0.048	1 x 10 <sup>-4</sup>	-	1.4 x 10 <sup>22</sup>	-	-0.3	-	0.75, 2μm	49
RhO	REACT VAC EVAP 125°C	192-1600	0.0125	2 x 10 <sup>-3</sup> -2.4x10 <sup>-4</sup>	-	-	-	0.54-0.68	-	0.75, 2μm	178
SiO-Ag	SIM EVAP	10	-	-	-	-	-	-0.25	-0.3	0.95, 10μm	163

TABLE 10. Continued

Material	Deposition Technique	Sheet Resistance ohm/sq	Thickness Microns	Bulk Resistivity ohm/cm	Mobility cm <sup>2</sup> /V-sec	Carrier Density cm <sup>-3</sup>	Bandgap eV	Ave T <sub>vis</sub>	T <sub>solar</sub>	R <sub>ir</sub> or (E <sub>ir</sub> )	Ref
SiO <sub>2</sub> -Ag	SIM EVAP	40	-	-	-	-	-	-0.4	-0.5	0.80, 10μm	163
TiN	PLAS REACT VAC EVAP, RT	~20-80	0.10-0.3	-6x10 <sup>-4</sup> -8x10 <sup>-4</sup>	-	-	-	-	-	-	172
Zn <sub>x</sub> Cd <sub>1-x</sub> S (x=0-0.3)	SIM EVAP 250°C	-10-5000	-4	2 x 10 <sup>-3</sup> -2	100-20	-	2.4-2.7	>0.75, 0.6μm	-	-	98
ZnO	VAC EVAP	47	0.2	9.4 x 10 <sup>-3</sup>	-	-	-	-	0.70, AM1*	-	164
ZnO	VAC EVAP	67	0.18	1.2 x 10 <sup>-3</sup>	-	-	-	-	0.74, AM1*	-	164
ZnO	VAC EVAP	82	0.3	2.5 x 10 <sup>-3</sup>	-	-	-	-	-	-	164

\* Without substrate

a Can also be sputtered at 100°C

films to provide a heat mirror effect in a double glazing and also it can be electrically heated to raise the temperature of the inner glazing, to control frost formation.<sup>99</sup>  $\text{Cu}_2\text{S}$  films appear promising as heat mirrors, except that the films must be protected since they exhibit low mechanical strength and are chemically unstable in humid or moist atmospheres.<sup>100</sup> Another related use for some of these materials is as nucleation layers for overcoating materials. The use of nucleation oxide layers has been investigated for deposition of Ag on polyester substrates.<sup>101</sup>

#### E. Metal Films and Metal Microgrids

Thin gold films (about 200 Å) for heat mirrors are favored over copper and silver due to their inertness to the environment,<sup>71,102,103</sup> as silver and copper readily form sulfides or oxides when exposed to air and atmospheric pollutants. However, silver films absorb the least amount of visible energy compared to Au and Cu. Better stability of Ag and Cu films can be achieved by overcoating with materials such as  $\text{Al}_2\text{O}_3$ ,  $\text{SiO}_2$ , SiC, and polymers.<sup>104,106,107,197</sup> The sheet resistance of a two-layer film can be calculated by:

$R_T = R_M R_D / (R_M + R_D)$ , where  $R_M$  and  $R_D$  are sheet resistances of the metal and dielectric films, respectively.

Also, metal films have been overcoated with semiconductors and dielectrics to suppress the high visible reflectance of the metal. Furthermore, overcoating with semiconductors serves to protect the thin metal layer from abrasion and atmospheric corrosion. An extension of the

overcoating idea is the multilayer film (see Sec. IV), which can be designed to be more broad-band with sharp transitions, and hence suitable for heat mirrors. There has been, however, some success with two-layer sputtered film heat mirrors. Thin metal films suffer from two inherent problems: agglomeration and surface roughening, resulting in diffuse scattering. To deposit thin continuous noble metal films, a nucleation modification compound is deposited prior to the metal film evaporating. Various oxides,  $\text{Bi}_2\text{O}_3$ ,  $\text{Au}_2\text{O}$ ,  $\text{Cu}_2\text{O}$ ,  $\text{NiO}$ ,  $\text{Al}_2\text{O}_3$ ,  $\text{CdO}$ ,  $\text{PbO}$ , and sulfides, tellurides, and selenides have been used with gold films. Also, for Ag, Cu, and Pt films,  $\text{Bi}_2\text{O}_3$ ,  $\text{Sb}_2\text{O}_3$ ,  $\text{MgF}_2$ ,  $\text{ZnO}$ ,  $\text{PbO}$ ,  $\text{Al}_2\text{O}_3$ , and  $\text{Cu}_2\text{O}$  have been used. The exact mechanism of the nucleation modification layer is not known; however, during various types of sputtering and evaporation the substrate is bombarded with electrons and hence negatively charged. This nucleation coating may act to provide a fresh dry surface that can be uniformly charged. Incoming positively charged metal ions will nucleate on the charged sites.

Both the optical and corrosion properties of Cu-Ni, Cr-brass, and Cr-Cu have been studied with overlayers of  $\text{SiO}_2$  and  $\text{Al}_2\text{O}_3$ .<sup>105</sup> Systems such as Ag/ $\text{SiO}_2$ , Cu/ $\text{SiO}_2$ , Ag/ $\text{Al}_2\text{O}_3$ , Cu/ $\text{Al}_2\text{O}_3$ , Brass/ $\text{SiO}_2$ , Brass/ $\text{Al}_2\text{O}_3$ , along with other metals have been investigated also.<sup>106,107</sup> Deposition was performed using custom ion beam sputtering apparatus. Table 2 details various metal films, and Figs. 18-19 show examples of reflecting thin metal films. Overcoated metal films are shown in Figs. 20-21. To increase scratch resistance of metal films, oxide co-deposit techniques using an electron beam

TABLE 2. THIN METAL AND OVERCOATED METAL FILMS

Material	Deposition Technique	Thickness, Angstroms	Sheet Resistance ohm/sq	Ave R <sub>vis</sub>	Ave T <sub>vis</sub>	R <sub>ir</sub> or (ε <sub>ir</sub> )	Ref
Ag	SPUT	260		0.82	0.13	0.09	119
Ag	VAC EVAP	260		0.86	0.21	0.15	119
Ag	PVD	100		-	-	0.41	165
Ag	VAC EVAP/REACT SPUT	100/350		-	-	-	166
Ag/In <sub>2</sub> O <sub>3</sub>	IB SPAT	-		0.23-0.35, 0.5μm	0.47-0.38, 0.5μm**	0.93, 2.5μm	106
Ag/Al <sub>2</sub> O <sub>3</sub>	IB SPAT	-		0.06, 0.5 μm	0.74, 0.5μm**	0.71, 2.5μm	106
Ag/Al <sub>2</sub> O <sub>3</sub>	IB SPUT	-		0.6-0.3, 0.5μm	0.15-0.29, 0.5μm	-	106, 107
Ag/SiO <sub>2</sub>	IB SPUT	-		0.06, 0.5μm	0.61, 0.5μm	0.69, 2.5μm	106
Ag/SiO <sub>2</sub> *	IB SPUT	-		-	-	-	166
Ag/ZnO	VAC EVAP/REACT SPUT	100/350		0.12, 0.56μm	0.55, 0.56μm	(0.35, 0.8-2μm)	116
Au	VAC EVAP	130		-	-	0.38	165
Au	VAC EVAP	100		-	0.3, 0.5μm	0.95, 10μm	8
Au	VAC EVAP	200		0.79	0.07	0.03	119
Au	SPUT	440		0.58	0.23	0.12	119
Au	VAC EVAP	440		0.17	0.12	0.34	108
Au-SiO <sub>2</sub>	EB RF SPUT	1200		-	-	-	167
(0.58, 0.42)	VAC EVAP ON NUC MOD	-	10-15	-	0.8	-	168
Au/Bi <sub>2</sub> O <sub>3</sub>	SPUT ON NUC MOD	-	10-15	-	0.8	-	166
Au/Bi <sub>2</sub> O <sub>3</sub>	VAC EVAP/REACT SPUT	100/350	-	-	-	0.075	105
Brass	RF SPUT	250	4.1	0.69	0.13	-	106
Brass/Al <sub>2</sub> O <sub>3</sub> *	IB SPUT	-	-	0.01-0.03, 0.5μm	-0.6, 0.5μm**	0.71-0.74, 2.5μm	106
Brass/SiO <sub>2</sub>	IB SPUT	-	-	0.13-0.45, 0.5μm	-0.21-0.5, 0.15μm	-0.99, 2.5μm	119
Cu	SPUT	220		0.48	0.24	0.13	119
Cu	EVAP	220		0.62	0.20	0.10	119

TABLE 2. Continued

Material	Deposition Technique	Thickness, Angstroms	Sheet Resistance ohm/sq	Ave R <sub>vis</sub>	Ave T <sub>vis</sub>	T <sub>solar</sub>	R <sub>ir</sub> or (E <sub>ir</sub> )	Ref
Cu, Zn-SiO <sub>2</sub> (0.58, 0.42)	EB RF SPUT	1200	-	0.37	0.23	0.40	(0.31)	108
Cu/SiO <sub>2</sub>	RF SPUT	220/960	-	0.38	0.23	0.12	0.97, 0.8-2μm	105
Cr	RF SPUT	30	-	0.16	0.60	0.58	0.14, 0.8-2μm	119
Cr	RF SPUT	50	-	0.32	0.33	0.36	0.23, 0.8-2μm	119
Cr	RF SPUT	200	-	0.68	0.06	0.08	0.55, 0.8-2μm	119
Cr	RF SPUT	94	-	0.56	0.12	0.13	-0.5, 2μm	105
Cr-SiO <sub>2</sub> (0.85, 0.15)	EB RF SPUT	300	-	0.28	0.42	0.50	(0.24)	108
Cr/Brass	RF SPUT	25/125	-	0.47	0.22	0.18	0.68, 0.8-2μm	105
Cr/SiO <sub>2</sub>	RF SPUT	94/960	-	0.30	0.14	0.14	-0.4, 2μm	105
Cr/Brass/SiO <sub>2</sub>	RF SPUT	10/200/670	-	0.75	0.14	0.09	0.92, 0.8-2μm	105
In	VAC EVAP -123°C	600-1000	5-200	-	0-0.5, 0.6μm	-	-	111
Rh:O	REACT VAC EYP 125°C	125	192-1600	-	0.54-0.68	-	-	178
Ti/ZnO	VAC EVAP	57/2000	41	-	-	-	-	164

\* On polyester or teflon

\*\* Measured from substrate side

Brass, Ni, Cu, Ti, Inconel, Mo, Au reflector layers have also been investigated.

## SPECTRAL SELECTIVITY OF METAL FILMS

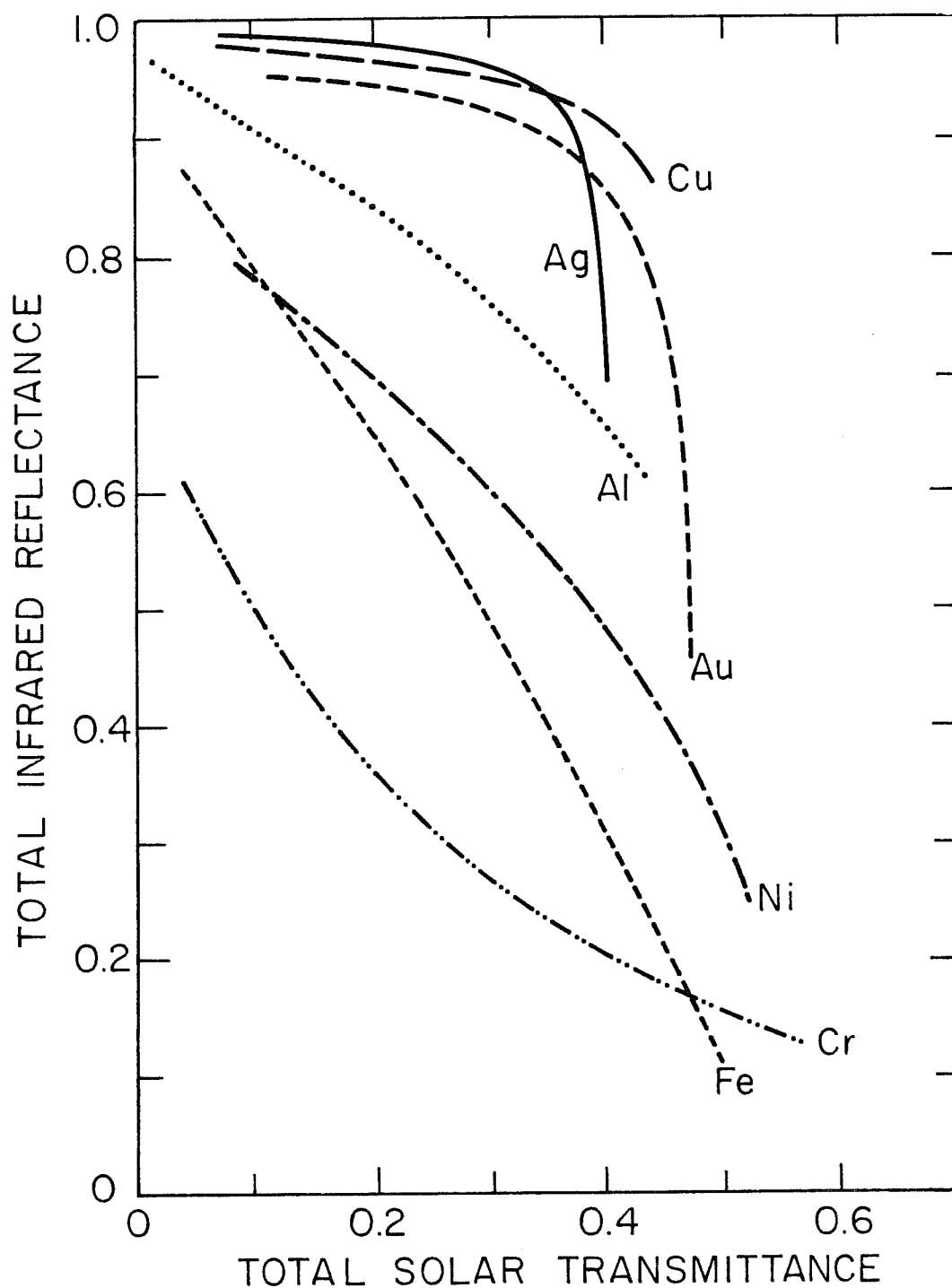
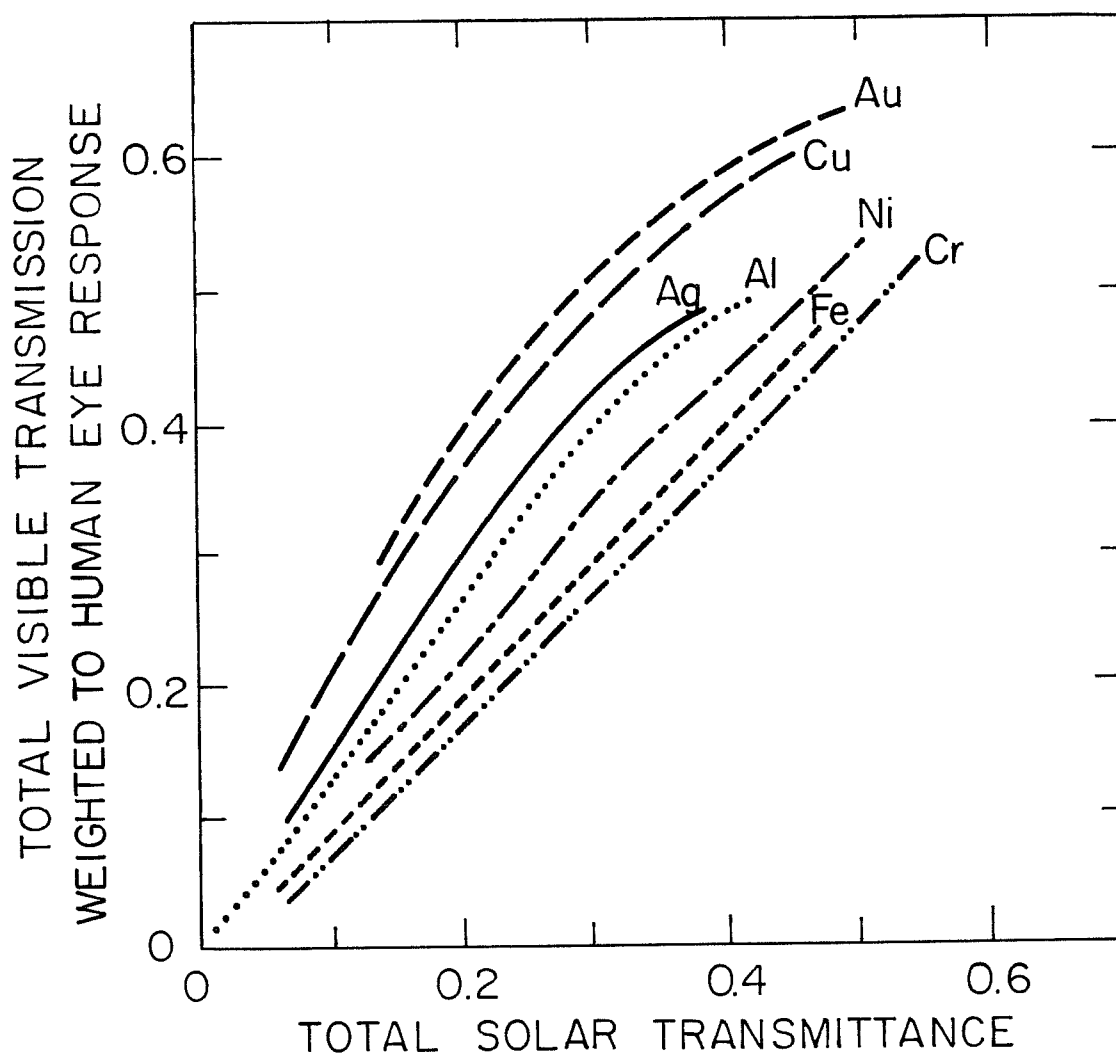


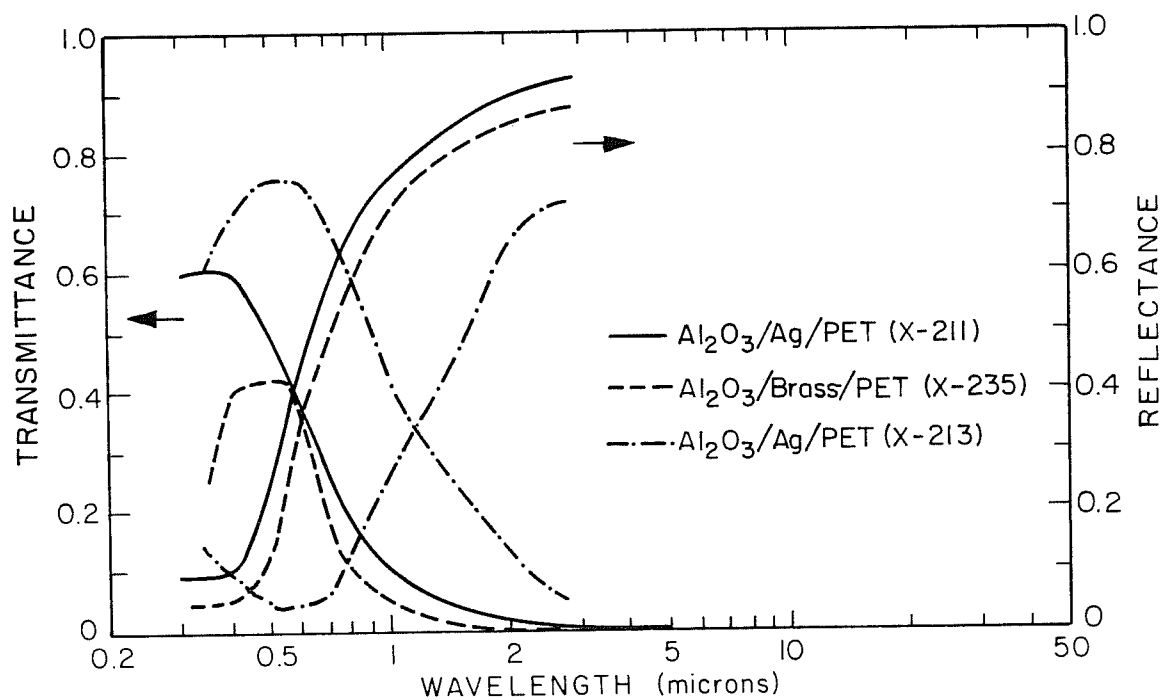
Fig. 18. Integrated infrared reflectance ( $10^{\circ}\text{C}$ ) as a function of transmitted total solar radiation for thin metal films of various thicknesses.<sup>122</sup> For Au, Fe, Cr films thickness ranges from 50–300 Å; Ni and Al films range 25–200 Å, and Ag and Cu films from 95–400 Å.

NEAR NORMAL ( $10^\circ$ ) TRANSMISSION PROPERTIES  
OF METAL FILMS



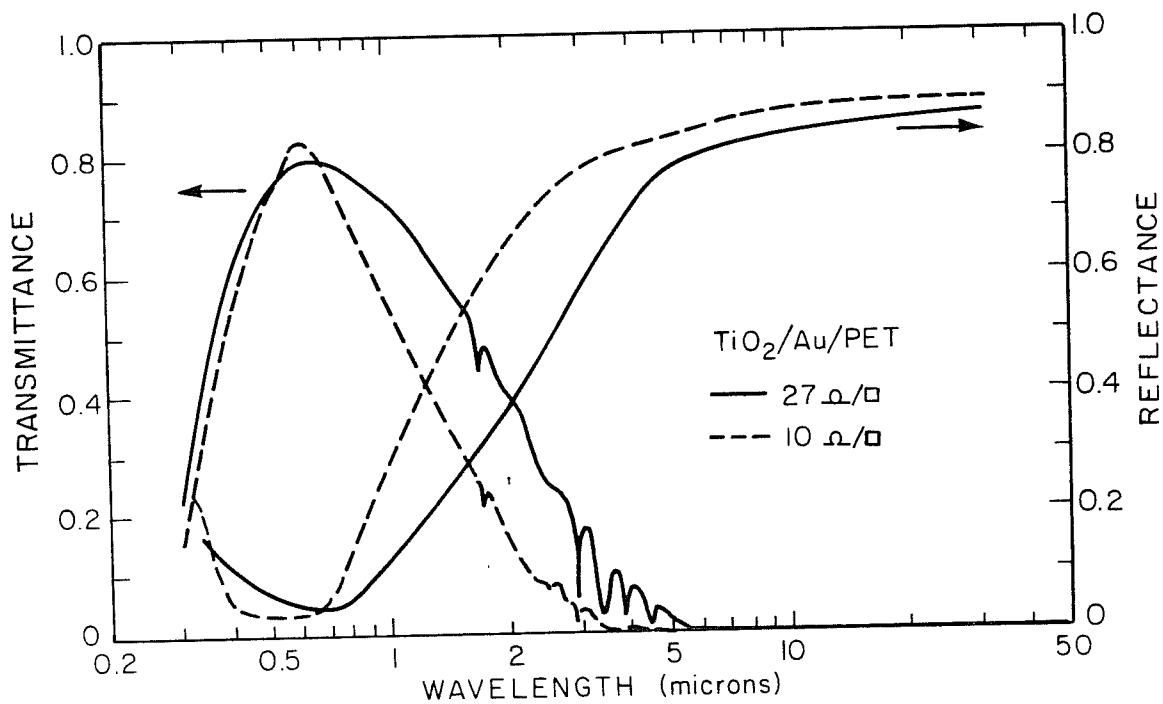
XBL 811-5091A

Fig. 19. Total visible transmission (weighted to the human eye response) as a function of total solar transmission for a range of metal films.<sup>122</sup>



XBL 814-5511

Fig. 20. Experimental films of Al<sub>2</sub>O<sub>3</sub>/metal on polyester (0.002"). It is shown that by design<sup>106</sup> the transition wavelength can be shifted to suit either a primary cooling or heating load reduction application.



XBL 814-5507A

Fig.21. Prototype heat mirror using TiO<sub>2</sub> overcoated gold films on polyester.<sup>123</sup> Deposition was performed by electron beam vacuum metalization in a roll coater. TiO<sub>2</sub> is formed by chemical deposition. The 27 ohm/sq film has  $T_{VIS} = .78$ ,  $T_{IR} = 0.01$ ,  $A_{IR} = 0.27$ ,  $R_{IR} = 0.72$ . The 10 ohm/sq coating exhibits  $T_{VIS} = 0.795$ ,  $R_{IR} = 0.87$ ,  $A_{IR} = 0.13$ .

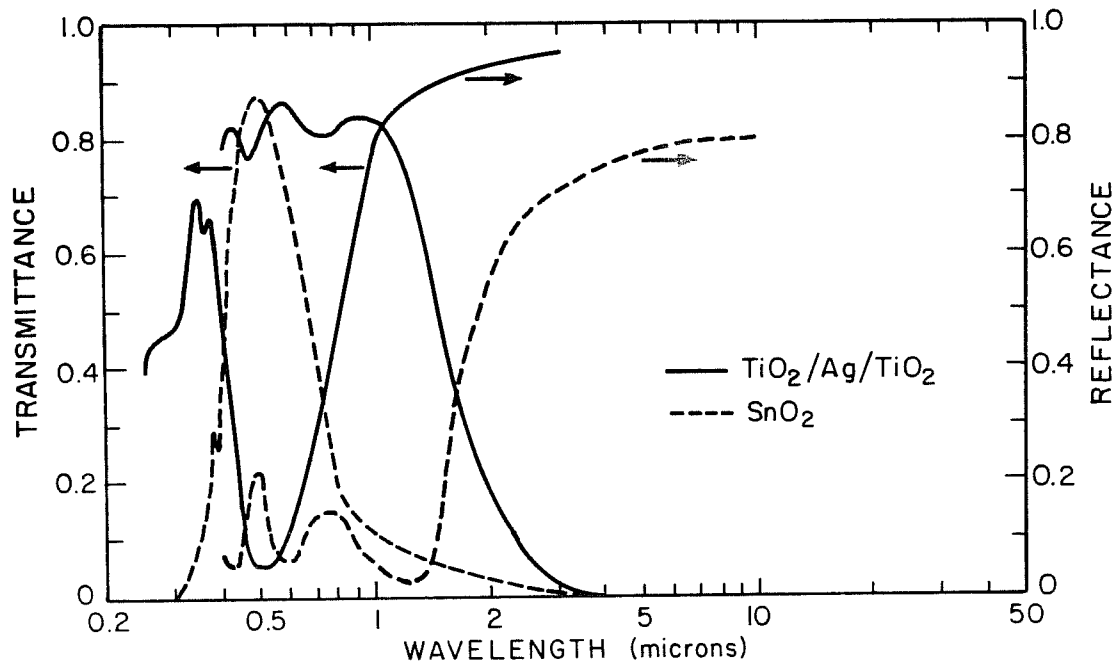
sputtering system can be used.<sup>108</sup> Systems that were evaluated ranged from Cr-SiO<sub>2</sub>, Cu-SiO<sub>2</sub>, Au-SiO<sub>2</sub>, and brass - SiO<sub>2</sub>. As a result of this work, it was found that for Au and Cr addition of SiO<sub>2</sub> showed increased IR transmission and reduced visible reflectance. Overall it shows that this approach gave durable films, but the heat mirror properties are degraded. Durable films of Ni-Cr have been made for neutral density filters.<sup>109</sup> Electroless reduction using a replacement reaction has been devised for Cu-Ag films on architectural glass.<sup>110</sup>

Transparent indium films have been made by PVD at low temperatures (150°K).<sup>111</sup> Electrical continuity is observed in films greater than 0.2 microns thick. The visible transmission is  $T_{vis} = 0.5$ . The melting point of indium is 157°C. Thin rhodium films can have improved transparency by adding oxygen during evaporation. Resistivities above  $1 \times 10^{-5}$  ohm-cm can be obtained for 100 Å films.<sup>112</sup> Rhodium is similar to chromium films in its chemical durability.

Pure metal microgrids can be used in the same way as heat mirror continuous films. The mesh, however, can give much higher transmittance in the visible and solar region. The microgrid appears to be reflective in the infrared by virtue of its mesh size. For wavelengths much greater than the mesh periodicity, the coating appears reflective. The mesh appears transparent for wavelengths close to the periodic spacing of the grid. Other considerations pertaining to the design of grid spacing and diameter have been studied.<sup>113</sup>

#### IV. MULTILAYER HEAT MIRROR FILMS

A selection of multilayer heat mirror films are presented in Table 3. Multilayer deposition of  $\text{TiO}_2/\text{Ag}/\text{TiO}_2$  has been performed by investigators at MIT for solar collectors<sup>63,71,114</sup> ( $\text{TiO}_2$  is a 3.2 eV semiconductor),<sup>170</sup> and later by Durotest, a light-bulb manufacturer. In the latter case the film was used to make a more energy efficient incandescent light bulb.<sup>8</sup> Examples in Fig. 22 show that the  $\text{TiO}_2$  film thickness is not a conventional  $1/4$  wavelength because the refractive index of  $\text{TiO}_2$  in the visible is larger than that of Ag.  $\text{TiO}_2$  has an refractive index of  $n = 2.2\text{--}2.65$  (visible range).<sup>117</sup> To make these films, the substrate is first ultrasonically cleaned in a commercial decontamination solution, rinsed in deionized water and blown dry with  $\text{N}_2$ . RF sputtering is performed after  $\text{TiO}_2$  target presputtering. The sample is sputtered with  $\text{TiO}_2$  in an Argon atmosphere ( $74 \text{ cm}^3/\text{min}$ ) at a pressure of  $7\text{--}10 \times 10^{-3}$  torr for 7.5 min at  $0.8 \text{ W}/\text{cm}^2$  potential, after which the Ag film is sputtered for 35 sec at  $0.4 \text{ W}/\text{cm}^2$  in argon. The last coating of  $\text{TiO}_2$  is then sputtered in the same way as the first.<sup>114</sup> It should be noted that the lack of presputtering in  $\text{Ar}/\text{O}_2$  gas yields inferior films. No degradation has been noted for these films when they were subjected to  $200^\circ\text{C}$  for 48 hours, and only small changes when subjected to  $300^\circ\text{C}$ . The coating thickness for a light bulb envelope is different from the conventional heat mirror coating.<sup>9</sup> The dielectric layers are  $340 \text{ \AA}$  and the silver layer  $240 \text{ \AA}$ , contrasted to the historical  $180 \text{ \AA}/180 \text{ \AA}/180 \text{ \AA}$  design.<sup>9</sup>



XBL809-5969A

Fig. 22. Optical properties of an energy-saving incandescent light bulb coating,<sup>8</sup>  $\text{TiO}_2/\text{Ag}/\text{TiO}_2$ . The  $\text{SnO}_2$  coating is used to improve the operation of low-pressure sodium lamps. This film was prepared by thermal spraying at  $460^\circ$  to a thickness of 0.32 microns.

By increasing these thicknesses effectively the transition wavelength is moved to shorter wavelengths to better reflect the near infrared.

The coating ZnS/M/ZnS (where M is some metal) has been optimized at 75–85 Å for Al, 100–150 Å for Ag, and 100–150 Å for Cu<sup>115</sup>; whereas the optimum thickness for the ZnS film was found by experiment to be 650 Å upper layer and 520 Å lower layer. Also, this system is stated to be useful with polymer substrates.<sup>115</sup> This coating is applied by physical vapor evaporation techniques. To increase durability of the ZnS/M/ZnS system, substitutions of  $\text{In}_2\text{O}_3\text{:Sn}$ ,  $\text{Bi}_2\text{O}_3$ , or  $\text{TiO}_2$  are generally considered; however, still other dielectrics can be devised.<sup>39</sup>

Prior British research looked at the  $\text{Bi}_2\text{O}_3/\text{Au}/\text{Bi}_2\text{O}_3$  multilayer coating, their only disadvantage being a yellowish coloration.<sup>116</sup> An interesting note here is that  $\text{Bi}_2\text{O}_3$  was sputtered in oxygen and gold evaporated under vacuum.<sup>116</sup> The major use for these heat mirrors was as lamp filters. The same investigators worked with  $\text{SiO}/\text{Au}$  films and obtained good films, but reported that the gold was less thermally stable in this system than it was with  $\text{Bi}_2\text{O}_3$ . Summarized data on this system and others is tabulated in Table 3.

## V. CONCLUSIONS

Rapid parallel progress of advanced deposition technology and fundamental understanding of both metal oxide and metallic film properties has resulted in a wide range of acceptable heat mirror materials. Furthermore, the increased international concern for energy

TABLE 3. MULTILAYER HEAT MIRROR COATINGS

Material	Deposition Technique	Thickness, Angstroms	Sheet Resistance ohm/sq	Ave $R_{vis}$	$T_{solar}$	$k_{ir}$ or $(\epsilon_{ir})$	Ref
$Bi_2O_3/Au/Bi_2O_3$	VAC EVAP	80/65/80	30	0.73, 0.56 $\mu m$	-	0.50, 0.8-2 $\mu m$	116
$Bi_2O_3/Au/Bi_2O_3$	VAC EVAP	80/100/80	10	0.71, 0.56 $\mu m$	-	0.64, 0.8-2 $\mu m$	116
$Bi_2O_3/Au/Bi_2O_3$	VAC EVAP	450/130/450	7	0.73, 0.56 $\mu m$	-	0.74, 0.8-2 $\mu m$	116
$SiO_2/Au/SiO_2$	RF SPUT	200/130/200	4	0.68, 0.56 $\mu m$	-	0.87, 0.8-2 $\mu m$	116
$TiO_2/Ag/TiO_2$	RF SPUT in Ar	180/180/180	-	0.84	0.54 <sup>a</sup>	(0.017, 121°C)	71, 135
$TiO_2/Ag/TiO_2$	RF SPUT	330/130/330	-	-	>0.72 <sup>a</sup>	0.95, 10 $\mu m$	135
$TiO_2/Ag/TiO_2$	RF SPUT in Ar	340/240/340	-	-0.7	-	0.98, 2.5 $\mu m$	9, 117
$ZnS/Ni/ZnS$	VAC EVAP	520/95/650	85	-	0.49	(0.35)	115
$ZnS/Ni/ZnS$	VAC EVAP	550/110/750	15	-	0.63	(0.11)	115
$ZnS/Ag/ZnS$	VAC EVAP	520/100/770	10	-	0.68	(0.06)	115, 173, 174
$ZnS/Ag/ZnS$	VAC EVAP	520/150/750	-	-	0.64	-	115, 173, 174
$ZnS/Al/ZnS$	VAC EVAP	520/75/650	50	-	0.49	(0.18)	115
$ZnS/Al/ZnS$	VAC EVAP	520/85/700	40	-	0.49	(0.16)	115
$ZnS/Ag/ZnS$	VAC EVAP	1090/180/1090	-	0.54, 0.56 $\mu m$	-	0.98±0.01, 3-15 $\mu m$	176

\* Can be used with polymer substrates

<sup>a</sup> Includes glass substrate

conservation in buildings, coupled with the development of other solar technologies (solar collectors and photovoltaics), has given heat mirror material research and development high importance.

Of the semiconductor single-layer materials,  $\text{In}_2\text{O}_3:\text{Sn}$ ,  $\text{Cd}_2\text{SnO}_4$ , and doped  $\text{SnO}_2$  are the traditional favorites. All of the optical properties of these films compete well for window applications. In terms of resource limitations and economics,  $\text{Cd}_2\text{SnO}_4$  and doped  $\text{SnO}_2$  are the most competitive. For low sheet resistance (1–10 ohm/sq)  $\text{In}_2\text{O}_3:\text{Sn}$  and  $\text{Cd}_2\text{SnO}_4$  are favored; however, improved  $\text{SnO}_2$  films can be competitive within this range. The major emphasis with all these coatings is on simplification and reduction of deposition time—two parameters that are too often inversely related. A major cost reduction comes from eliminating the post-annealing cycle. To make matters more difficult, more polymer substrates are being considered that require low deposition temperatures. For such substrates, the proper film morphology and chemistry is best achieved by plasma-activated processes such as ion plating. Another issue germane to high-rate processing is the potential influence of a rapidly moving substrate upon the resulting film properties, such as supersaturation. The bulk of the research thus far has been with static substrates.

Chemical vapor deposition is still widely used to deposit metal oxides on glass. Atmospheric pressure conveyor furnaces are used for continuous processing. CVD techniques tend to be simple and economical compared to PVD processes. By plasma enhancement, substrates held at room temperature can be coated. Further work is needed to optimize the

effects of plasma activation. Unenhanced CVD is generally limited to high temperatures, 400–700°C (glass and refractory substrates), although lower temperature reactions may be devised. With the use of high temperatures, there are problems of secondary competing reactions, such as alkaline substrate reactions. It is very important for the various dominant and limiting CVD reactions to be identified and understood in terms of chemical thermodynamics and kinetics. The development of low-cost organometallic feedstock chemicals can give CVD further advantages over other processes.

Innovative chemical dip processes may offer very inexpensive, versatile heat mirror or overlayer filtering abilities. These processes should not be ignored for higher technology solutions.

There is still much room for the development of heat mirror materials of the doped semiconductor type, and not limited to oxide types. Certainly, all the binary systems which have high visible transparency and high conductivity and mobility haven't been covered. Other material systems of ternary (like  $\text{Cd}_2\text{SnO}_4$ ) and higher order systems are virtually unexamined.

Unprotected metal films simply do not offer the stability and durability required of practical heat mirrors. Overcoated metals and dielectric/metal/dielectric films do offer excellent spectral properties with some tunability of the effective transition wavelength. One of the major concerns with these systems are their long-term durability of the dielectric layers that protect the metal films. Questions of interdiffusion, permeability, and interfacial reactions need to be

answered. Perhaps new films formed by plasma polymerized, plasma-enhanced processes may play an important role here.

Large-scale coaters (3x3 meter substrates) of both the batch evaporative and sputtering type are in operation, along with numerous roll-coating metallizers. Currently, some systems are useful and others need to be modified to accommodate the current heat mirror deposition techniques. This might mean incorporation of low-temperature roll coating or fast batch processing using plasma enhancement. Of course, before doing so, better understanding and control of processing parameters as they relate to optimum film properties are required. This necessitates the study of chemistry and microstructure of these films with correlation to basic mechanisms of deposition in terms of thermodynamics and kinetics of nucleation and growth, including defect formation. Structure-property studies are of the utmost importance.

Further considerations must include durability of films in their operating environment, whether it be a window or a solar device. This consideration complicates matters by bringing film studies into the realm of atmospheric oxidation, corrosion, erosion, and pollutant reactions, indoors and out.

In the long term, heat mirrors may have switchable properties, so that continuous energy optimization may be utilized. Optical shutter materials such as photochromic, thermochromic, and electrochromic films are under investigation for this purpose.<sup>118</sup>

## VI. ACKNOWLEDGMENTS

The author would like to express his appreciation to the various cited researchers and manufacturers who have provided material for this study. A special thanks goes to my research group colleagues for supporting this effort: Steve Selkowitz, Sam Berman, Jack Washburn, Mike Rubin, and Joe Klems.

The work described in this paper was supported by the Assistant Secretary for Conservation and Renewable Energy, Office of Buildings and Community Systems, Buildings Division of the U.S. Department of Energy under Contract No. W-7405-ENG-48.

### General Notes about Accuracy of Tabulated Data

All data tabulated has been extracted from research reference papers or lectures. In certain cases, values are selected from graphical relationships or from data too numerous to cite completely. Generally, data is chosen to reflect lowest bulk resistance or sheet resistance with high  $T_{vis}$  or  $T_{solar}$ . Tabulated data does not generally represent all of the author's developments and current research, or any unpublished work. The material published here generally has not been verified by each author represented. Optical data may contain substrate losses, as many authors do not state whether or not the substrate was compensated for when  $T$ ,  $R$  values were measured. These tables should be used as guides to the literature.

### Key to Table Notations

a	- amorphous structure
ANN,T	- annealed at temperature T
c	- crystalline structure
CONV FURN	- conveyor furnace
CVD	- some type of chemical vapor deposition technique, generally hydrolysis or pyrolysis
DC SPUT	- direct-current sputtering
CYL	- cylindrical magnetron
EB	- electron beam
IB SPUT	- ion-beam sputtering
OXIDE	- oxide target used in sputtering
ON NUC MOD	- process performed with nucleation modification layer
PH, T	- preheat at temperature T
PLAS REACT SPUT	- plasma-assisted reactive sputtering (ion plating)
PLAS REACT VAC DEP	- plasma-assisted reactive sputtering (ion plating)
REACT SPUT	- reactive sputtering in $O_2$ -containing atmospheres
REACT VAC EVAP	- reactive vacuum evaporation in $O_2$ -containing atmospheres
RF SPUT	- radio frequency sputtering
RT	- substrate held at or near room temperature
SIM EVAP	- simultaneous evaporation from two or more sources
SP HYDRO	- spray hydrolysis CVD
SP PYRO	- spray pyrolysis CVD
VAC EVAP	- vacuum evaporation and condensation process
~	- approximate or estimated value

## REFERENCES

1. S. Selkowitz, Proc. of 3rd Passive Solar Conf., "Transparent Heat Mirrors for Passive Solar Heating Applications," San Jose, California, January 1979. (LBL-7833)
2. H. Kostlin, Philips Tech. Rev. 34 (1974) 242.
3. S. Yoshida, Appl. Opt. 17 (1978) 145.
4. R.D. Goodman and A.G. Menke, Solar Energy 17 (1975) 207.
5. M. Matsuda, Terada, Toyota R/D 6 (1980) 27.
6. J.H. Apfel, J. Vac. Sci. Technol. 12 (1975) 1016.
7. T. Feng, A.K. Ghosh, C. Fishman, J. Appl. Phys. 50 (1979) 4972.
8. S.A. Spura et al., Opt. Spect. March (1980) 57.
9. S.A. Spura et al., Paper 17, Proceedings of Illumination Engineering Society Conference, Atlantic City, New Jersey, 1979.
10. G. Hass, J.B. Heany, and A.R. Toft, Appl. Optics 18 (1979) 1488.
11. S. Selkowitz, Proc. of 3rd Passive Solar Conf., "Daylighting and Passive Solar Buildings," San Jose, California, January 1979. (LBL-8825)
12. S.E. Selkowitz, ASRAE Trans. 85.2 (1979) 669.
13. M. Rubin, R. Creswick, and S. Selkowitz, "Transparent Heat Mirror for Windows: Thermal Performance," Proceedings of the 5th National Passive Solar Conference, Amherst, Mass., October 1980.
14. Suntek Research Assoc., "An Energy Efficient Window System," Lawrence Berkeley Lab report (LBL-9307), August 1977.

15. M. Rubin, Int. J. of Energy Res., to be published 1981; also, LBL-12246, February 1981.
16. F. Mahdjuri, Energy Res. 1 (1977) 135.
17. R. Groth, W. Reichelt, Gold Bull. 7 (1974) 62.
18. P.O. Jarvinen, J. Energy 2 (1978) 95.
19. J.N. Avaritsiotis, R.P. Howson, Thin Solid Films 65 (1980) 101.
20. G.L. Ruth, G. Krogseng, and R. Weiher, "Transparent Insulation--A New Inner Glazing Material," Proc. of Solar Glazing Conf., Atlantic City, New Jersey, 1979.
21. H. Dislich, E. Hussman, Thin Solid Films 77 (1981) 129.
22. S. Kulaszewicz, I. Lasocka, C. Michalski, Thin Solid Films 55 (1978) 283.
23. N. Gralenski, Proc. of Annual American Ceramic Society Meeting, 1980.
24. J.M. Blocher, Jr., Thin Solid Films 77 (1981) 51.
25. J. Kane, H.P. Schweizer, W. Kern, J. Electrochem. Soc. 123 (1976) 270.
26. T.R. Viverito, E.W. Rilee, and L.H. Slack, Am. Ceram. Soc. Bull 54 (1975) 217.
27. R. Gordon, Harvard University, private communication.
28. E. Leja, A. Kolodziej, T. Pisarkiewicz, and T. Stapinski, Thin Solid Films 76 (1981) 283.
29. F.H. Huang, H.B. Huntington, Phys. Rev. B9 (1974) 1479.

30. M. Buchanan, J. Webb and D. Williams, Appl. Phys. Lett. 37 (1980) 213.
31. R.P. Howson, J.N. Avaritsiotis, M.I. Ridge, C. Bishop, Thin Solid Films 63 (1979) 163.
32. R.P. Howson et al., 4th Int. Thin Film Cong., "Reactive Ion Plating of Metal Oxides onto Insulating Substrates," Loughborough, England (1978).
33. R.P. Howson, J.N. Avaritsiotis, M.I. Ridge, C. Bishop, Appl. Phys. Lett. 35 (1979) 161.
34. M.I. Ridge, M. Stenlake, R.P. Howson, and G.A. Bishop, Thin Solid Films, to be published July 1981.
35. J.C.C. Fan, Appl. Phys. Lett. 34 (1979) 515.
36. H.S. Randhawa, M.O. Matthews, and R.F. Bunshah, Thin Solid Films, to be published in 1981.
37. S.K. Ghandi, R. Sivig, J.M. Borrego, Appl. Phys. Lett. 34 (1979) 833.
38. G. Kienel and H. Walter, R/D Nov (1973) 49.
39. G. Kienel, Thin Solid Films 77 (1981) 213.
40. K. Peschmann, J. Calow, K. Knauff, J. Appl. Phys. 44 (1973) 2252.
41. S. Berman, S. Silverstein, in Efficient Use of Energy, No. 25, (H.C. Wolfe, Ed.), American Institute of Phys., 1975, p. 245.
42. C.M. Lampert, Solar Energy Mat. 1 (1979) 319.
43. B.O. Seraphin, A.B. Meinel, in Optical Properties of Solids, New Developments (B.O. Seraphin, Ed.), North Holland, Amsterdam, 1976, p. 927.

44. C.E. Wickersham and J. Greene, Phys. Status Solidi 47 (1978) 329.
45. D. Gross, Thin Solid Films 77 (1981) 128.
46. V.A. Baum and A.V. Sheklein, Geliotekhnika 4 (1968) 50.
47. G. Haacke, Ann. Rev. Mat. Sci. 7 (1977) 73.
48. W.W. Molzen, J. Vac. Sci. Technol. 12 (1975) 99.
49. V. Hoffman, Optical Spectra 12 (1978) 60.
50. E. Kaganovich, V.D. Ovsjannikov, S.V. Svechnikov, Thin Solid Films 60 (1979) 33.
51. P.J. Clarke, J. Vac. Sci. Tech. 14 (1977) 141.
52. H. Hoffmann, A. Dietrich, J. Pickl, Appl. Phys. 16 (1978) 381.
53. H. Hoffmann, J. Pickl, M. Schmidt, Appl. Phys. 16 (1978) 239.
54. W.R. Sinclair et al., J. Electrochem. Soc. 112 (1965) 1096.
55. J.C.C. Fan and F.J. Bachner, J. Electrochem. Soc. 122 (1979) 1719.
56. J.C.C. Fan and J.B. Goodenough, , J. Appl. Phys. 48 (1977) 3524.
57. J.R. Bosnell and Waghorne, Thin Solid Films 15 (1973) 141.
58. W.G. Haines, R.H. Bube, J. Appl. Phys. 49 (1979) 304.
59. Y. Ohhata, F. Shinoki, S. Yoshida, Thin Solid Films 59 (1979) 255.
60. W. Pawlewicz and N. Laegreid, Proc. of SPIE 140 (1978) 156.
61. J.A. Thornton, V.L. Hedgcoth, J. Vac. Soc. Tech. 13 (1976) 117.
62. M. Just, N. Maintzer, and I. Blech, Thin Solid Films 48 (1978) L19.
63. K. Itoyama, J. Electrochem. Soc. 126 (1979) 691.
64. R.P. Howson and M.I. Ridge, Thin Solid Films 77 (1981) 119.
65. J. Kane, H.P. Schweizer, W. Kern, Thin Solid Films 29 (1975) 155.
66. A. Raza, O. Agnihotri, and B. Gupta, J. Phys. D10 (1977) 1871.

67. S. Kulaszewicz, Thin Solid Films 74 (1980) 211.
68. J-C. Manificier et al., Mat. Res. Bull. 14 (1979) 109.
69. J.L. Vossen, RCA Rev. 32 (1971) 289.
70. H. Kostlin, R. Jost, W. Lems, Phys., Status Solidi A 29 (1975) 87.
71. J.C.C. Fan, F.J. Bachner, Appl. Optics 15 (1976) 1012.
72. C.M. Horwitz, Opt. Commun. 11 (1974) 210.
73. J.C.C. Fan, F.J. Bachner, and R.A. Murphy, Appl. Phys. Lett. 28 (1976) 440.
74. H. De Waal and F. Simonis, Thin Solid Films 77 (1981) 253.
75. A.V. Sheklein, Geliotekhnika 3 (1967) 84.
76. Z.M. Jarzebski, J.P. Marton, J. Electrochem. Soc. 123 (1976) 199C.
77. Z.M. Jarzebski, J.P. Marton, J. Electrochem. Soc. 123 (1976) 299C.
78. Z.M. Jarzebski, J.P. Marton, J. Electrochem. Soc. 123 (1976) 333C.
79. J. Sanz Maudes and T. Rodriguez, Thin Solid Films 69 (1980) 183.
80. M. Mizuhashi, Thin Solid Films 76 (1981) 97.
81. H. Watanabe, Jpn. J. Appl. Phys. 9 (1970) 1551.
82. R. Kalbskopf, Thin Solid Films 77 (1981) 65.
83. J. Cognard, C. Ganguillet, and Y. Ruedin, Abst. of Coatings on Glass 1980, Geneva, Switzerland.
84. R. Pommier, C. Gril, and J. Marucchi, Thin Solid Films 77 (1981) 91.
85. R. Muto and S. Furuuchi, Rept. Res. Lab. Asahi Glass Co. 23 (1973) 27.
86. R. Muto and S. Furuuchi, Oyo Buturi 41 (1972) 134.
87. M. Hecq, A. DuBois, J. Van Cakenberghe, Thin Solid Films 18 (1973) 117.

88. A.F. Peterson, "The Electrical Properties of Tin Oxide, PhD thesis, Rutgers, University Microfilms Intern., 1968.
89. A. Rohatyi, T. Viverito, and L.H. Slack, "Reviews on High Temperature Materials" 3 (1976) 139; J. Am. Ceram. Soc. 57 (1974) 278.
90. A.F. Carroll and L.H. Slack, J. Electrochem. Soc. 123 (1976) 1889.
91. E. Leja, T. Pisarkiewicz, A. Kolodziej, Thin Solid Films 67 (1980) 45.
92. O.P. Agnihotri, B.K. Gupta, A.K. Sharma, J. Appl. Phys. 49 (1978) 4540.
93. A.J. Nozik, Phys. Rev. B6 (1972) 453.
94. G. Haacke, A. Phys. Lett. 28 (1976) 622.
95. G. Haacke, W.E. Mealmaker, L.A. Siegel, Thin Solid Films 55 (1978) 67.
96. S. Maniv, C. Miner, and W. Westwood, "High Rate Deposition of Transparent Conducting Films by Modified Reactive Planar Magnetron Sputtering of  $\text{Cd}_2\text{Sn}$  Alloy," presented at Vac. Soc. Meeting, Detroit, Michigan, October 1980.
97. D. Hall, J. Electrochem. Soc. 124 (1977) 804.
98. N. Romeo, G. Sberveglieri, and L. Tarricone, Appl. Phys. Lett. 32 (1978) 807.
99. L.N. Anufriev and B.M. Melamed, Geliotekhn. 14 (1978) 48.
100. V.P. Kryzhanovskii, Opt. i Spec. 24 (1968) 135.
101. C. Bishop, R. Howson, and M. Ridge, Thin Solid Films 72 (1980) 341.

102. R. Cornely, N. Fuschillo, J. Vac. Sci. Tech. 11 (1974) 163.
103. R.H. Cornely and T.A. Ali, J. Appl. Phys. 49 (1978) 4094.
104. M.J. Wadlinger and L.M. Garcia, Proc. of the Solar Glazing Materials Conf., Atlantic City, NJ, 1979.
105. B. Lalevic, G. Taylor, and W. Slusark, Thin Solid Films 39 (1976) 143.
106. W.J. King. "High Performance Solar Control Windows," Lawrence Berkeley Lab report (LBL-12119), 1981.
107. W.J. King, "High Performance Solar Control Office Windows," Lawrence Berkeley Laboratory report (LBL-7825), December 1977.
108. G. Taylor, B. Lalevic, W. Slusark, Thin Solid Films 39 (1976) 165.
109. M. Banning, J. Opt. Soc. Am. 37 (1947) 686.
110. C.B. Greenberg, J. Electrochem. Soc. 123 (1976) 337.
111. D.K. Murti, J. Vac. Sci. and Tech. 16 (1979) 226.
112. D. Hoffman and M.D. Coutts, J. Vac. Sci. Technol. 13 (1976) 122.
113. D. Pramanik, A. Sievers, and R. Silsbee, Solar Energy Materials 2 (1979) 81.
114. G. Frank, E. Kauer, H. Kostlin, Thin Solid Films 77 (1981) 107.
115. M.M. Koltun, S.A. Faiziev, Geliotekhnika 10 (1974) 58.
116. L. Holland, G. Siddall, Brit. J. of Appl. Phys. 9 (1958) 359.
117. G. Hass, Vacuum 11 (1952) 331.
118. C.M. Lampert, Electrochromic materials for energy efficient windows (LBL-10862), to be published in J. Elect. Mat.
119. N. Fuschillo, Solar Energy 17 (1975) 159.

120. S. Sobajima et al., Jap. J. Appl. Phys. Sup. 2 pt 1 (1974) 475.
121. G. Haacke, A. Phys. Lett. 30 (1977) 380.
122. B. Karlsson, C.G. Ribbing, Technical Report of the Inst. of Technol., Contract 3879-1, Uppsala, Sweden, 1978.
123. B.P. Levin and P.E. Schumacher, "A Discussion of Heat Mirror Film: Performance, Production Process, and Cost Estimates," Lawrence Berkeley Lab report (LBL-7812), October 1977.
124. B.P. Kryzhanovskii, Opt. i Spec. 10 (1961) 682.
125. J.C. Manifacier, J. Fillard, and J. Bind, Thin Solid Films 77 (1981) 67.
126. T. Nagatomo and O. Omato, Oyo Butsuri 47 (1978) 618.
127. R. Groth, Phys. Status Solidi 14 (1966) 69.
128. H.J.J. vanBoort, R. Groth, Philips Tech. Rev. 29 (1968) 18.
129. G. Blandenet, M. Court, and Y. Lagarde, Thin Solid Films 77 (1981) 81.
130. E. Kawamata, K. Oshima, Jpn. J. Appl. Phys. 18 (1979) 205.
131. D. Furuuchi, Proc. of Microelect. Soc. Jap. Meeting, 1973.
132. E. Kauer, Phil. Tech. Rev. 26 (1965) 33.
133. D.B. Fraser and H.D. Cook, J. Electrochem. Soc 119 (1972) 1368.
134. P.J. Clarke, J. Vac. Sci. Tech. 14 (1977) 141.
135. J.C.C. Fan, Optics in Solar Energy Utilization II, Vol. 85, SPIE, Bellingham, Washington, 1977, p. 39.
136. Y. Ohhata and S. Yoshida, Oyo Butsuri 46 (1977) 43.
137. R.R. Mehta and S.F. Vogel, J. Electrochem. Soc. 119 (1972) 752.

138. J.C.C. Fan, F. Bachner, and G. Foley, Appl. Phys. Lett. 31 (1977) 773.
139. J.M. Pankratz, J. Elect. Mat. 1 (1972) 182.
140. T. Nishino, Y. Hamakawa, Jpn. J. of Appl. Phys. 9 (1970) 1085.
141. K. Ishiguro et al., J. Phys. Soc. Jap. 13 (1958) 296.
142. B.J. Baliga, S.E. Ghandi, J. Electrochem. Soc. 123 (1976) 941.
143. A.B. Meinel, M.P. Meinel, Applied Solar Energy, an Introduction, Addison Wesley, Reading, Mass., 1976, p. 282.
144. M. Mizuhashi, Thin Solid Films 70 (1980) 91.
145. A.R. Peaker, B. Morsley, Rev. Sci. Instrum. 42 (1971) 1825.
146. P. Nath and R.F. Banshah, Thin Solid Films 69 (1980) 63.
147. J. Smith, A. Aronson, D. Chen, and W. Class, Thin Solid Films 72 (1980) 469.
148. P. Nath, R. Bunshah, B. Basol, and O. Staffsuo, Thin Solid Films 72 (1980) 463.
149. J. Kane, H.P. Schweizer, and W. Kern, J. Electrochem. Soc. 122 (1975) 1144.
150. G. Haacke, H. Ando, W.E. Mealmaker, J. Electrochem. Soc. 124 (1977) 1923.
151. N. Miyata, K. Miyake, T. Fukushima, K. Koga, Appl. Phys. Lett. 35 (1979) 542.
152. P. Lloyd, Thin Solid Films 41 (1977) 113.
153. N. Miyata, K. Miyake, J.J. Appl. Phys. 17 (1978) 1673.

154. M. van der Leij, "Spectral-Selective Surfaces for the Thermal Conversion of Solar Energy" (PhD thesis) Delft University Press, Delft, The Netherlands, 1979.
155. R.P. Howson, Int. Coatings Conf., San Diego, California, 1980.
156. T.K. Lakshmenan, J. Electrochem. Soc. 110 (1963) 548.
157. S. Kulaszewicz, Thin Solid Films 76 (1981) 89.
158. N. Romeo, G. Sberveglieri, and L. Tarricone 55 (1978) 413.
159. C. Pan and T. Ma, Appl. Phys. Lett. 37 (1980) 163.
160. N. Miyata, K. Miyake and Y. Yamaguchi, Appl. Phys. Lett. 37 (1980) 180.
161. S. Couve et al., Thin Solid Films 15 (1973) 223.
162. V.P. Kryzhanovskii, Opt. i Spec. 25 (1968) 343.
163. V.P. Kryzhanovskii, A. Kuznetsov, and L. Palomova, Opt. i Spec. 15 (1963) 447.
164. P. Petron, R. Singh, and D.E. Brodie, Appl. Phys. Lett. 35 (1979) 930.
165. R. Groth and E. Kauer, Philips Tech. Rev. 26 (1965) 105.
166. J.L. Vossen, Phys. of Thin Films 9 (1977) 1.
168. L. Holland, G. Siddall, Vacuum 3 (1953) 375.
169. E.J. Gillham, J.S. Preston, B.E. Williams, Phil Mag. 46 (1955) 1051.
169. J.N. Avaritsiotis and R.P. Howson, Thin Solid Films 77 (1981) 351.
170. P.A. Kohl, S.N. Frank, A.J. Bard, J. Electrochem. Soc. 124 (1977) 225.

171. J.C.C. Fan, F.J. Bachner, G.F. Foley, and P.M. Zavracky, Appl. Phys. Lett. 25 (1974) 693.
172. Y. Murayama, J. Vac. Sci. Technol. 12 (1975) 818.
173. M.M. Koltun, S.A. Faiziev, U.K. Gaziev, Geliotekhnika 12 (1976) 43.
174. L.B. Panfilova and V.F. Skachkov, Opt. i. Spec. 37 (1974) 440.
175. C.A. Pan and T.P. Ma, J. Elect. Mat. 10 (1981) 43.
176. B. Bhargava, R. Bhattacharyya, V. Shah, Thin Solid Films 40 (1977) 29.
177. W. Slusark, Jr., B. Lalevic, and G. Taylor, Thin Solid Films 39 (1976) 155.
178. D.M. Hoffman, J. Vac. Soc. Technol. 13 (1976) 122.
179. C.M. Lampert, Solar Energy Mat. 2 (1979) 1.